Detailed mapping of the Upper Hutchinson Salt and Overlying Permian strata beneath Hutchinson, Kansas

Open-file Report No. 2003-66

Susan E. Nissen and W. Lynn Watney

Introduction

In response to the January 2001 natural gas explosions and geysers in Hutchinson, KS, 57 vent wells and five observation wells were drilled in the city of Hutchinson and westward towards the Yaggy natural gas storage facility (Fig. 1), which had experienced a leak in a well, S-1, two days prior to the explosions. At Yaggy, natural gas is stored at depths in excess of 600 ft in solution-mined caverns in the Hutchinson Salt Member of the Lower Permian Wellington Formation of the Sumner Group. An estimated 143 million cubic feet of gas escaped from a casing leak above the storage cavern, at a depth of approximately 600 ft. Vent wells were drilled to intercept the gas and, in all but one of the productive wells, the gas was confined to an interval approximately 170 ft above the Hutchinson Salt, informally called the 3-finger dolomite. The zone was named from the pattern formed by the close succession of three low natural gamma ray intervals as seen on correlation logs, corresponding to three thin dolomite beds as observed in core. The 3-finger dolomite is believed to be equivalent to the Milan Limestone Member, at the top of the Wellington Formation. DDV #64, in T23S R6W Sec. 3, is unique in that, on July 7, 2001, it suddenly vented large amounts of gas at high pressure over several days. This gas originated from another zone 70 ft below the 3-finger dolomite as interpreted from gas shows and log response. This lower zone has a series of low gamma ray beds similar to the log response of the 3-finger dolomite.

Most of the vent wells penetrated into the Hutchinson Salt, providing a substantial amount of new data on the distribution of the upper Hutchinson Salt and overlying layers at a high degree of spatial resolution. Natural gamma-ray logs from these wells and 59 nearby oil wells and gas-storage wells were used to conduct high-resolution stratigraphic correlation and mapping of 15 closely-spaced marker beds within the Permian strata for a 150-mi^2 area encompassing Hutchinson and Yaggy. Preliminary mapping conducted as relief wells were drilled suggested patterns in structure and deposition that appeared to have influenced the migration of subsurface gas in the Hutchinson area. The work reported in this paper was undertaken later to extend the area mapped and increase the well control in order to refine the structural and stratigraphic distribution of a more finely resolved succession of stratigraphic units. The objective was to improve the understanding of the geologic history just prior to, during, and subsequent to the deposition of the 3-finger dolomite.

Ten marker beds were defined and correlated within the Ninnescah Shale and upper Wellington Formation (Fig. 2), including the top and base of the 3-finger dolomite and the M1A marker, which corresponds to the lower gas zone in DDV #64. Also, the top of

the Hutchinson Salt Member (S1) and four marker beds within the upper Hutchinson Salt Member were correlated within the study area. The S2 marker is equivalent to the regional CM5 marker, and the S4 marker is equivalent to the regional CM4 marker of Watney et al. (1988). At the eastern edge of the study area, the S1, S2, and S3 salt markers correlate with thinner beds exhibiting higher natural gamma ray intensity (M5, M6, and M7, respectively), suggesting that the uppermost salt in this area may have undergone a lateral facies change associated with the depositional edge of the salt basin (Fig. 6).

All maps were constructed in Petra using triangulation and a least squares gridding algorithm.

Structure

Structure maps for 13 of the Permian marker beds, as well as the configuration of the base of the Quaternary Equus Beds, which unconformably overly the Permian strata in the study area, are shown in Figure 3. All of the structure maps show a regional westerly dip of approximately 15-20 ft/mi. Locally, the structure maps show a 1.5-2.5 mi wide zone of structural flattening of the monoclinal westerly dip, centered on a local high in T23S R6W Sec. 3 (at the location of DDV #64). This feature also serves to define the apex of a subtle anticline referred to as the Yaggy-Hutchinson anticline, which extends in an E-W direction from Yaggy to western Hutchinson.

The base of Equus Beds configuration (Figure 3N) is inferred to represent the erosional base of a paleo-incised valley paralleling the Arkansas River, centered approximately 2-3 miles to the south of the present river within the study area. The map illustrates part of a large trunk stream that passes through the Hutchinson area described more fully in Watney et al. (2003). Tributaries draining from north of the modern Arkansas River in the vicinity of Hutchison closely follow subjacent paleotributary valleys that drain into the more deeply incised primary trunk stream of the paleo-Arkansas River. Other depositional and stratigraphic correlations to this paleoriver system are examined in this report.

The Arkansas River follows a distinctively linear course through the area over a distance of 90 miles. In turn, the river valley corresponds closely to the paleo-Arkansas River drainage. Moreover, a linear trend of productive vent wells follows the crest of an anticline between Hutchinson and Yaggy that closely parallels the Arkansas River. These coincidences provided the motivation to evaluate their possible interrelationships and common structural origin, and to use the combined information to help constrain the model to explain the subsurface gas migration in Hutchison.

Isopachs

Isopach maps were created for 12 stratigraphic intervals lying between a series of Permian marker beds (Figure 4). The smaller isopach intervals represent successions of thin beds of shale, gypsum, carbonate, and halite based on core and outcrop data. Ideally,

isolation of sedimentary packages such as time-distinct depositional sequences could have been used to map temporal stratigraphic changes to infer sedimentary and structural processes that caused them. However, long cores from this interval were not available to establish the depositional sequences. Thus nearly equi-spaced stratigraphic intervals between log markers were chosen for the mapping and interpretation.

The salt isopachs (S3/M7-S4, S2/M6-S3/M7, and S1/M5-S2/M6) and the M4-S1/M5 isopach are discussed in detail in Watney et al. (2003). In summary, the S3/M7-S4 isopach (Figure 4A) shows only minor changes in thickness throughout the study area. There is an apparent subtle overall thinning towards the south and west, possibly due to variations in salt and shale deposition. The S2/M6-S3/M7 isopach (Figure 4B) shows little variation in thickness over most of the study area, but abrupt eastward thinning along a 1-mile-wide north-northeast trending wedge in central Hutchinson. Salt dissolution is suggested as the cause of this abrupt thinning. This dissolution edge parallels and lies approximately 5 miles west of the main dissolution front of the Hutchinson Salt. The main salt dissolution front closely corresponds to the crest of the Voshell Anticline east of Hutchinson. The north-northeast trend of the main dissolution front extends southward until the front reaches the Arkansas River, where it abruptly turns southeast following the Arkansas River to near Wichita, a distance of approximately 40 miles (Watney et al., 2003).

In the area of abrupt thinning of the S2-S3 interval, the overlying S1/M5-S2/M6 isopach (Figure 4C) thickens by up to 8 ft, suggesting that the accommodation space for the upper salt bed may have been formed by early, interformational dissolution of the underlying layer prior to deposition of the S1-S2 interval. The S1/M5-S2/M6 isopach also shows abrupt eastward thinning in the eastern part of the study area, approximately 0.7 mi east of the thinning in the underlying halite interval as well as a broad, but distinctive, zone of thinning along the Arkansas River to the south and west of Hutchinson, minor thinning parallel and to the north of the Yaggy-Hutchinson anticline, and a minor north-northeast trending thin at the western edge of Hutchinson. The north-northeast trend at the western edge of Hutchinson corresponds with the edge of a tributary valley reflected in the map of the base of Equus Beds configuration (Figure 3N). These areas of northwesterly and north-northeasterly trending thinning of a halite-dominated interval are ascribed to salt dissolution, and possibly depositional thinning along the eastern edge of the study area. Depositional thinning is suggested by a concordant change in log expression suggesting an apparent facies change in the interval, e.g. from halite to gypsum to carbonate (Figure 6B).

Intervening dissolution, desiccation, and minor erosion occurring between halite cycles are suggested in nearby cores and underground mines, including the mine at Hutchinson where lower portions of the Hutchinson Salt are mined. These apparent intraformational subaerial exposure events probably reflect corresponding episodic falls in sea level, exposing at least this landward edge of the evaporate basin. The marine sabkha model also predicts the landward facies change from halite to gypsum to carbonate to shale as suggested by log cross sections extending east of Hutchinson (Watney et al., 2003).

An isolated thick in the S1/M5-S2/M6 isopach forms a distinctive rhombic-shaped area, centered on Hutchinson, bordered on the east by a northeasterly trending thinning due to dissolution that again parallels the Voshell Anticline, on the south by northwesterly trending thinning due to dissolution that closely follows the course of the Arkansas River, and on the west by a less distinctive zone of thinning between Hutchinson and Yaggy. The isolated thick may represent greater preservation of evaporites bounded by areas of dissolution.

The M4-S1/M5 interval (Figure 4D) shows an area of thickening (approximately 6 ft) corresponding to the area of thinning (approximately 16 ft) in the S1/M5-S2/M6 isopach situated beneath the Arkansas River south and west of Hutchinson. This local elongated thickening suggests that some of the S1/M5-S2/M6 salt dissolution was early, and that the resulting accommodation space developed on the land surface was filled by deposition of M4-S1/M5. The remaining 10 ft of thinning in the S1/M5-S2/M6 isopach is interpreted to have occurred at a later time, most likely post-Permian (Watney et al., 2003).

Between M4 and L2, Watney et al. (2003) display isopachs for intervals between significant markers only. These isopachs are shown in Figure 5, and can be compared with the isopachs of their subdivisions shown in Figure 4.

The M1A-M4 isopach (Figure 5A) is significantly thinner in the center of the study area than to the west and southeast. Most of this variation is contained in the M3-M4 isopach (Figure 4E), particularly the thickening at the west side of the study area. A localized, circular thin, about one mile in diameter, centered on T23S R6W Sec. 10, is seen on the M2-M3 isopach (Figure 4F), but with less magnitude than for the M1A-M4 isopach, indicating that there is also subtle thinning at this location in the M3-M4 and M1A-M2 (Figure 4G) isopachs. The subdivided isopachs also reveal trends that are not observed on the composite isopach suggesting that changes are sporadic and are rapidly compensated for in superjacent strata. Thus, isopach intervals can be sufficiently large to preclude resolution of these important stratigraphic events. For instance, the M1A-M2 isopach shows a subtle band of northwest-southeast trending thinning running through the center of the study area. Within this trend, there is additional thinning in T23S R6W Sec. 3, corresponding to the location of DDV #64. It is possible that this localized thinning at DDV #64, at the center of a local structural high, is linked in some way to sudden venting of gas from DDV #64 in July 2001, six months after the initial explosions. Such localized thinning may be associated with focused dissolution of evaporites, collapse, and natural fracturing, with sufficient disruption of the stratigraphic column to carry pressured gas from one dolomite rich interval to another.

The M1-M1A isopach (Figure 4H) shows a broad, subtle L-shaped thick, which runs north-south through central Hutchinson to the north of the Arkansas River, and then bends to the southeast to parallel the Arkansas River. This thick also dominates the composite Top 3-finger-M1A isopach (Figure 5B). The Top 3-finger-M1 isopach (Figure 4I) shows a subtle thin with apparently similar shape, which is located to the west of the thick in the M1-M1A isopach. The thickest part of the Top 3-finger-M1 isopach is at the

western side of the study area, although there is not enough well control to uniquely define the shape of this thick. The sharp bend in the isopach trend for these intervals indicates possible structural control on sedimentation along intersecting north-south and northwest-southeast lineaments. Both the north-south, and northwesterly trends have already been identified in the S2/M6-S3/M7, S1/M5-S2/M6, and M4-S1/M5 isopach maps, with evaporite dissolution being invoked as a possible explanation for these trends of thinning. The Base Equus configuration map, depicting erosional topography of an incised valley system, shows similar north-northeasterly and northwesterly trends that may be associated with underlying structural controls, i.e., fracture/joint trends in Permian bedrock, the focus of this current study. Watney et al. (2003) relate these possible structural trends to two regional structures: the Voshell Anticline (north-south to northeast-southwest) and the Arkansas River Lineament (northwest-southeast). Fractures, subtle uplift or subsidence, and local dissolution of evaporites probably combined to create the observed patterns in these isopach maps. Episodic movement along structures may have resulted in increased fracture density, continuity, or aperture size and accordingly may have allowed undersaturated waters to come in contact with evaporites leading to locations of preferred dissolution.

The L2-Top 3-finger isopach (Figure 5C) is dominated by variations in the L2-D1 isopach (Figure 4K). In contrast, the D1-Top 3-finger isopach (Figure 4J) is very uniform in thickness throughout most of the study area, except for local thickening along the eastern side of the study area. The north-northwest trending thin through the center of the study area in the L2-D1 isopach (Figure 4K) appears to have been an area of locally reduced sedimentation. The isopach map of the G2-L2 interval overlying L2-D1 shows a corresponding thickening in the same area, suggesting infilling of the previous area of thinning (Figure 4L).

Lithology

Natural gamma ray serves as an indicator of lithology when substantiated with nearby core or outcrops. Since not all gamma-ray logs in the study area were scaled in API units, the gamma-ray logs were normalized to vary from 0 (salt) to 100 (shale). The minimum and maximum gamma values used in the normalization were obtained from an interval extending from 20 ft above the top 3-finger dolomite to 100 ft below the top Hutchinson salt. Mean normalized gamma values were extracted for 9 intervals from D1 to S3 and are displayed in map view in Figure 5. Mean gamma was not extracted for stratigraphic intervals above D1, because of varying depths to the casing shoe above this marker. Steel casing generally reduces the gamma ray response of the logging tool and casing collars further reduce the signal, thus limiting the use of gamma ray data in cased intervals for quantitative purposes. .

The mean normalized gamma ray maps of the S2/M6–S3/M7 (Figure 6A) and S1/M5-S2/M6 (Figure 6B) intervals show fairly uniform low gamma over most of the mapped area, indicating that these intervals are primarily comprised of halite. Increased gamma values along the eastern mapped area are related to facies changes in the halite beds, believed to reflect the depositional limit of the halite along the margins of the Hutchinson

Salt evaporite basin (Watney et al., 1988). For the S2/M6-S3/M7 interval, there is also an increase in the mean gamma associated with the thinning of the isopach below 6 ft, most likely an artifact of the tool resolution.

Within the upper Wellington Shale above the top of Hutchinson salt (S1), normalized gamma ray shows that the shaliest mapped interval is between the base of the 3-finger dolomite and M1. The cleanest interval (lowest gamma) is M4-S1/M5, just above the top of Hutchinson salt.

All of the intervals between S1 and D1 appear to show a northwest-southeast-trending band of lower gamma ray which follows the trend of gas-producing vent wells in the middle of the survey area. This feature is most pronounced for M1A-M2 (Figure 6F), where the trend is also seen in the isopach map. For M4-S1/M5 (Figure 6C), a north-south-trending band of low gamma is superimposed on the northwest-southeast trend.

Elevated gamma radiation of a thinner interval may reflect the reduction of cleaner evaporite through localized dissolution and relative increase in shale content, e.g., along the northwest-southeast thinning at the center of the S1-S2 isopach. Areas of lower gamma ray and interval thickening may suggest greater preserved evaporite or thicker carbonate, e.g., the S1-S2 thick centered on Hutchinson. Higher gamma ray and a thicker interval may relate to a greater proportion of clastics in place of evaporites or carbonate strata, e.g., the southwestern edge of the M3-M4 maps and the western and northeast portions of the top 3-finger-M1 maps.

The 3-Finger Dolomite Interval

An isopach of the 3-finger dolomite (Figure 7A) shows it to be between 17 and 20 ft thick throughout most of the study area, with no clear thickening or thinning trend.

Variations in lithology of the 3-finger dolomite interval were investigated by looking at maps of mean normalized gamma ray (Figure 7B) and minimum normalized gamma ray (Figure 7C). Because dolomite is brittle and fracture-prone in contrast to shale and evaporites, which are in general more ductile, dolomite is likely to undergo induced fracturing and be able to maintain open fractures when subjected to high-pressure gas that exceeds the fracture pore pressure of the dolomite. An increase in the amount of gypsum and shale, both less brittle than dolomite, would tend to inhibit fracturing and prevent migration of gas, thus, the focus of gas flow through the 3-finger dolomite as indicated by the gas bearing vent wells.

Mean gamma (Figure 7B), which shows average shaliness of the interval, indicates that, in general, the 3-finger dolomite is cleanest along a northwest-southeast trending corridor from Yaggy to Hutchinson, including the city proper, with considerable increase in shaliness to the southwest and minor increase in shaliness to the northeast. Minimum gamma, which identifies the shaliness of the cleanest dolomite within the interval (the top dolomite in all but a few wells), shows an even more dramatic decrease beneath Hutchinson and along the corridor northwest of the city toward Yaggy. The areas of

lowest gamma ray in the 3-finger dolomite within and near the city are deemed more susceptible to fracturing and possibly have extant natural fractures that could serve as gas conduits, as the parting pressures of the extant fractures could be considerably lower than the pressure needed to create new fractures. Based on patterns of inferred evaporite dissolution and stream drainage patterns, joints and fractures appear to be related to both the northwesterly lineament of the Arkansas River and the north-northeasterly trending lineaments related to the Voshell Anticline. These lineaments underwent organized episodic movement as evidenced by the extended continuity (miles in length) of mapped trends of evaporite dissolution, facies change, and drainage patterns suggesting oriented, fracture clusters. Gas could migrate along these preferred fracture sets if parting pressures of the fractures were exceeded.

Conclusions

The structure, isopach, and mean normalized gamma ray maps reveal two major trends in the Lower Permian strata of the Hutchinson Area: northwest-southeast and north-south to northeast-southwest. The northwest-southeast trend is reflected in the configuration of the base of the Quaternary Equus Beds and the present-day Arkansas River drainage, and aligns with the Arkansas River Lineament (ARL). The north-south trend may be structurally controlled by the Voshell Anticline (Watney et al., 2003).

Variations in lithology, as inferred from maps of gamma ray intensity, do not always correspond to variations in the isopach maps, but appear to align with the northwest-southeast (and to a lesser degree, north-south) structural trends. Combinations of the gamma ray and isopach maps indicate plausible evidence for focused, oriented evaporite dissolution that corresponds with and parallels major lineaments identified in the area, the ARL and Voshell Anticline. Inferred episodic opening of fracture clusters along lineament boundaries perhaps facilitated temporary access of undersaturated water to beds containing evaporites leading to intermittent evaporite dissolution. Oriented fractures may have also provided weaknesses in the bedrock surface that offered a structural template as courses of stream drainages were defined. Subtle uplift and tilting associated with minor episodic structural movements, especially along the lineaments, may have also helped to define oriented depositional patterns inferred from isopach and gamma ray mapping. Structural reactivation in relationship to the local geology including basement heterogeneity is further described in Watney et al. (2003).

Combined high-resolution isopach and gamma ray mapping coupled with a knowledge of the lithofacies provides an effective means to resolve temporal changes in depositional and diagenetic patterns and trends that appear to be linked to significant structural lineaments. Structural activity along these lineaments is apparently episodic, and coarser stratigraphic mapping may leave this activity undistinguishable. The inferred structural deformation is at large enough scales (100’s of feet to miles) that it is also difficult to detect and characterize with localized studies or examination of limited outcrops. Yet, the potential impact of such structural lineaments on rock properties, particularly anisotropy, cannot be overestimated. High-resolution stratigraphic mapping at sufficient spatial

dimensions provides one approach to the detection and characterization of these structural lineaments.

References

Watney, W. L.; Berg, J. A.; and Paul, S. E., 1988, Origin and distribution of the Hutchinson Salt Member (lower Leonardian) in Kansas; *in*, Morgan, W. A.; and Babcock, J. A. (eds.), Permian rocks of the mid-continent: Society of Economic Paleontologists and Mineralogists, Midcontinent Section, Special Publication, no. 1, p. 113-135.

Watney, W. L.; Nissen, S. E.; Bhattacharya, S.; and Young, D., 2003, Evaluation of the role of evaporite karst in the Hutchinson, Kansas, gas explosions, January 17 and 18, 2001; in Johnson, K. S.; and Neal, J. T. (eds.), Evaporite karst and engineering/environmental problems in the United States: Oklahoma Geological Survey Circular 109, in press.

FIGURES

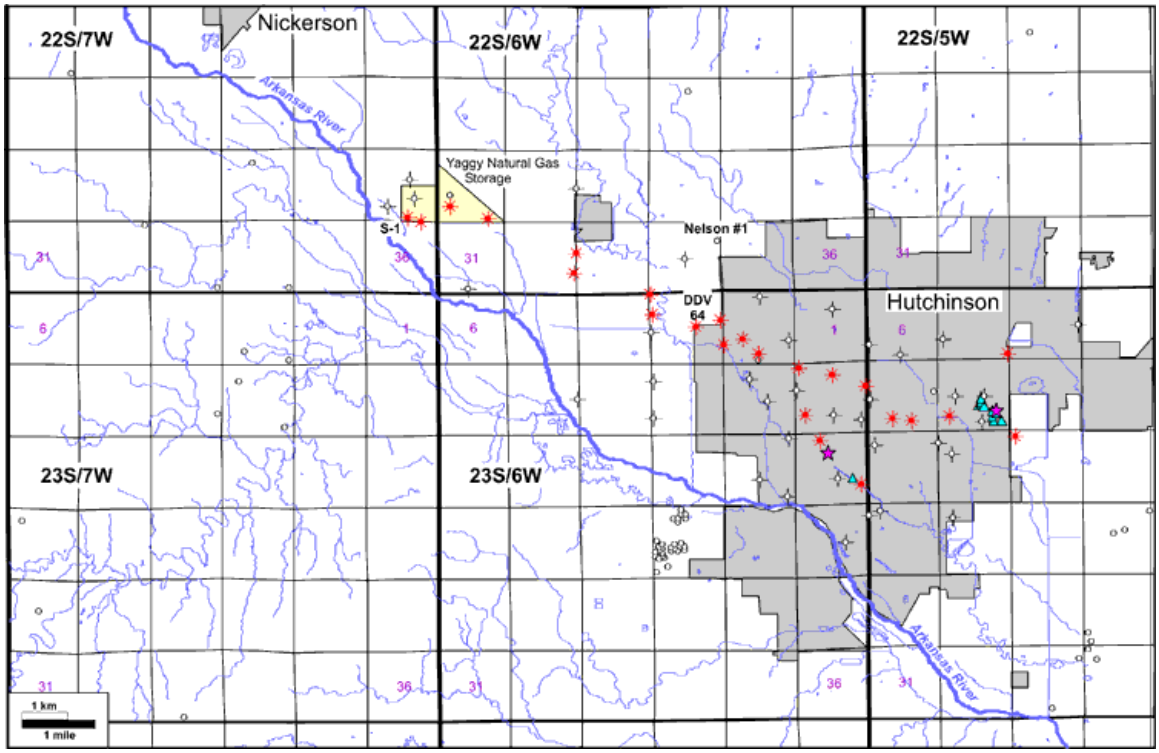

Figure 1. Base map of the study area. Locations of gas geysers are shown by blue triangles, and explosion sites are indicated by magenta stars. Observation and vent wells that vented natural gas are indicated by a red producing-well symbol. Vent wells that did not produce gas are indicated by a dry-hole symbol. Additional wells used for log correlations are shown with an open circle.

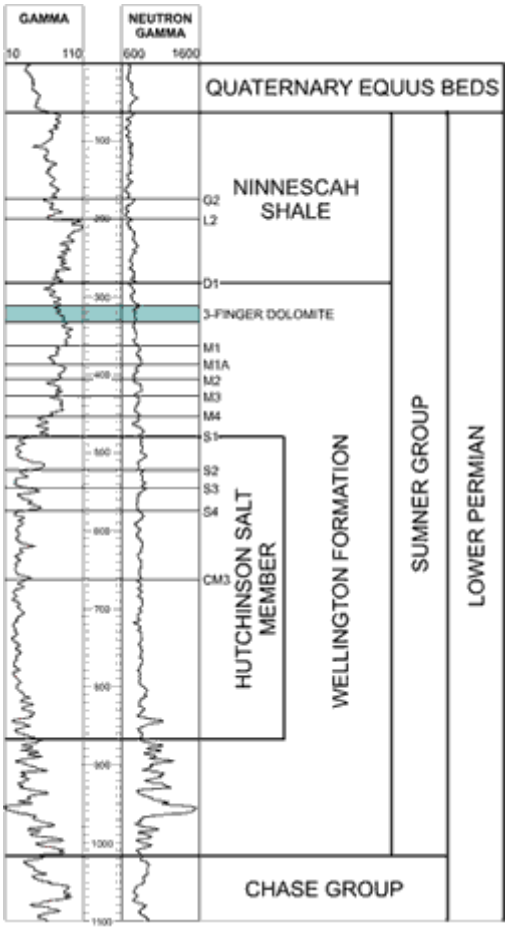

Figure 2. Natural gamma-ray and unscaled neutron-porosity logs from the Nelson #1 well in Sec. 34, T. 22 S., R. 6 W., showing distinctive log response of stratal members significant to study, including Lower Permian Leonardian-age Sumner Group containing the Hutchinson Salt Member of the Wellington Formation and the Ninnescah Shale, unconformably overlain by the Quaternary-age Equus Beds. Closely spaced marker beds G2 to S4 mapped in this study are shown as short horizontal lines. The regional CM3 marker bed mapped in Watney et al. (1988), which divides the upper and lower Hutchinson Salt Member, is also indicated.

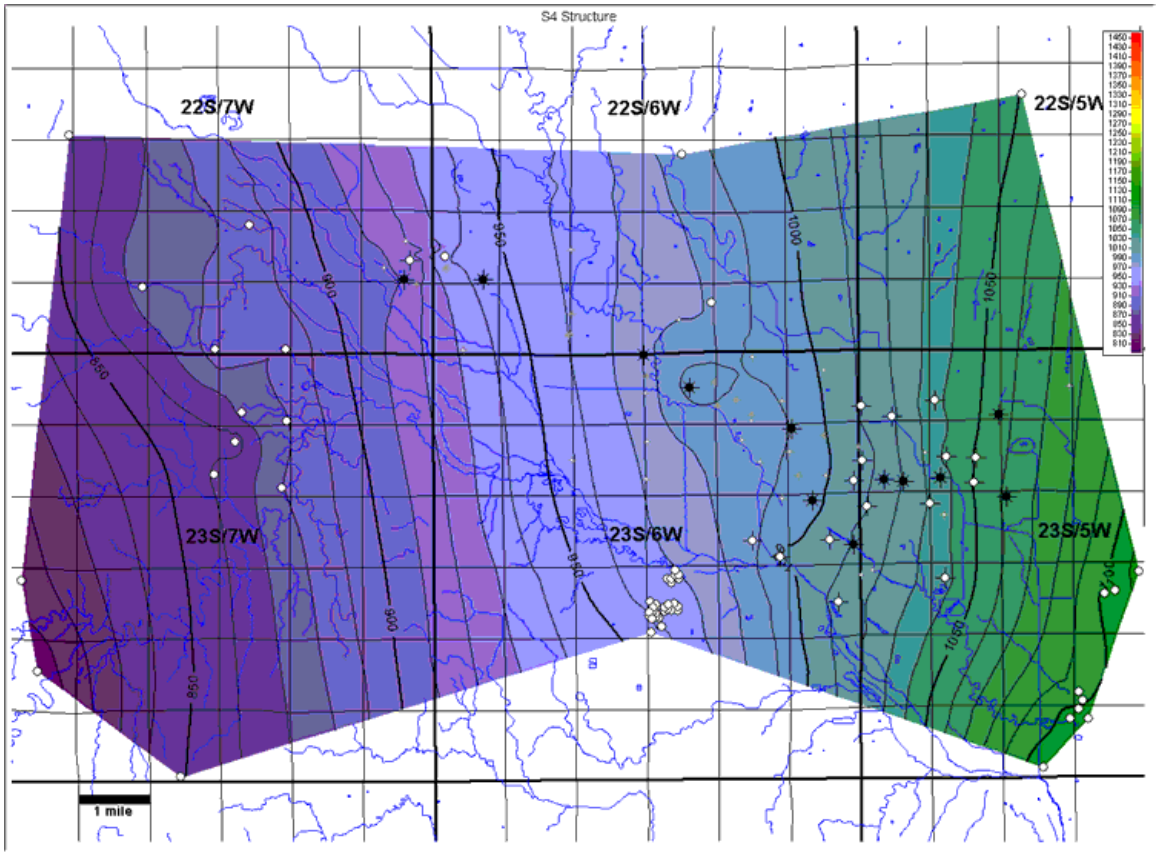

Figure 3A. Structure map of the S4 marker. Contour Interval = 10 ft. Wells within the study area not used in generating this map are displayed in gray at half size.

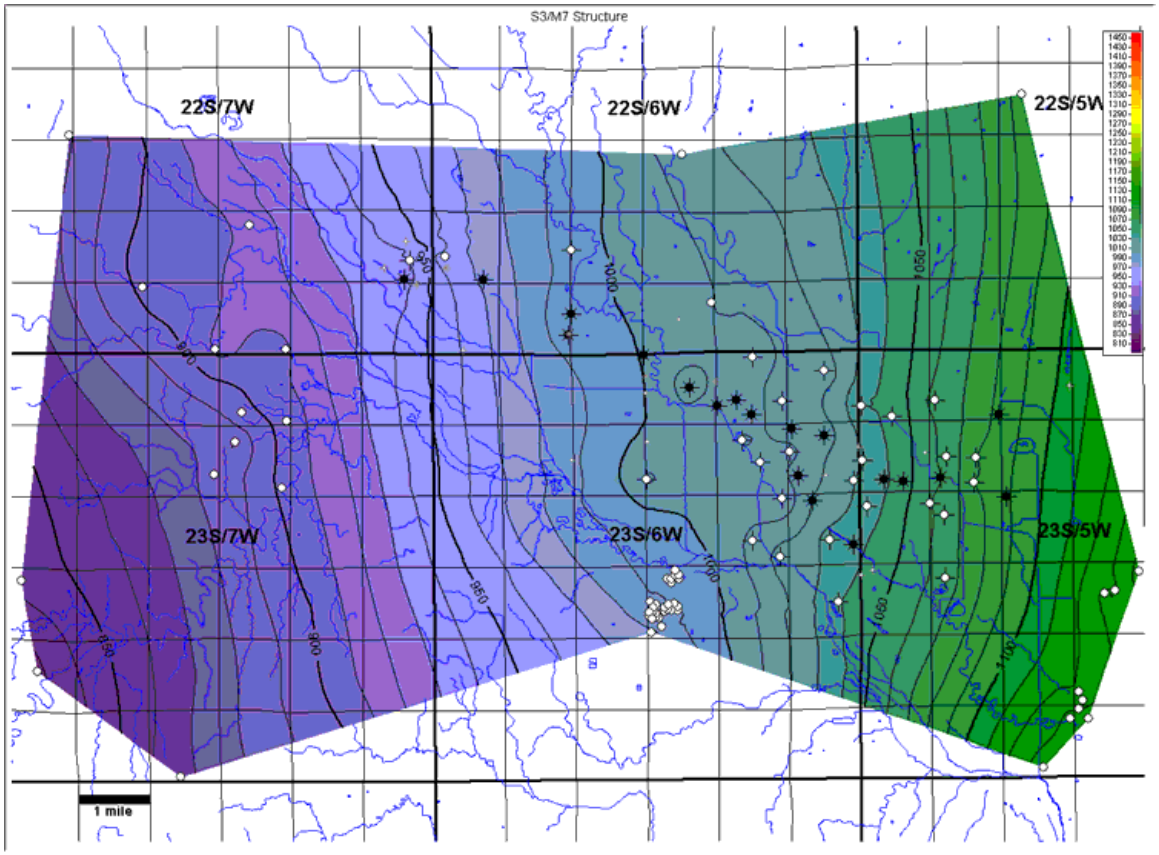

Figure 3B. Structure map of the S3 marker and laterally correlated M7 marker. Contour Interval = 10 ft. Wells within the study area not used in generating this map are displayed in gray at half size.

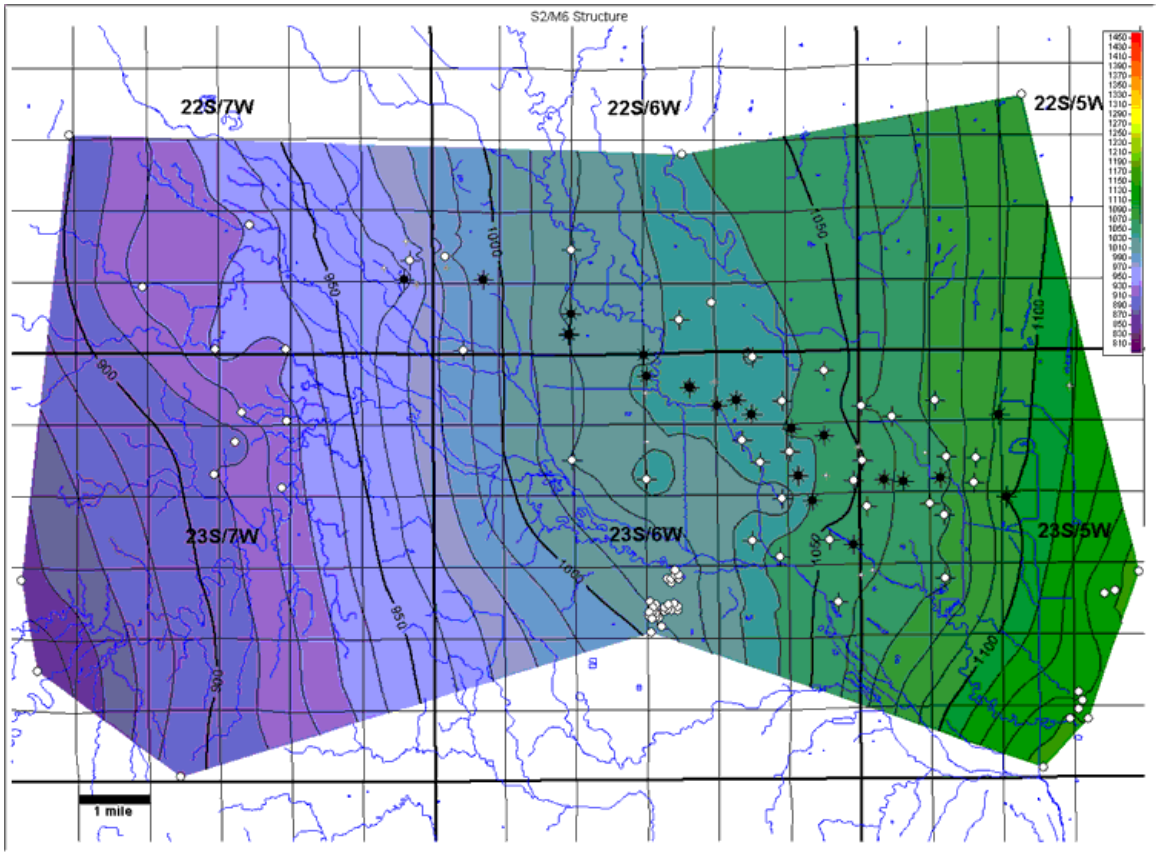

Figure 3C. Structure map of the S2 marker and laterally correlated M6 marker. Contour Interval = 10 ft. Wells within the study area not used in generating this map are displayed in gray at half size.

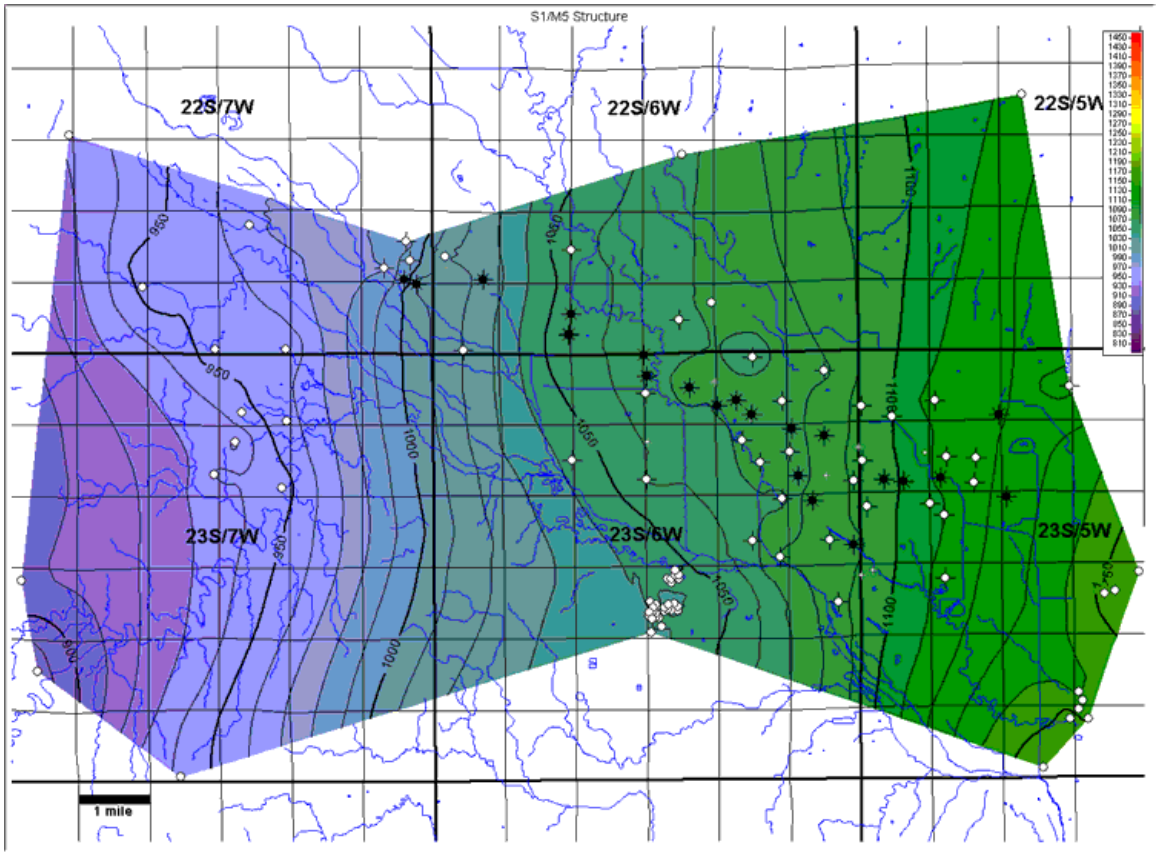

Figure 3D. Structure map of the Top of Hutchinson Salt Member (S1 marker) and laterally correlated M5 marker. Contour Interval = 10 ft. Wells within the study area not used in generating this map are displayed in gray at half size.

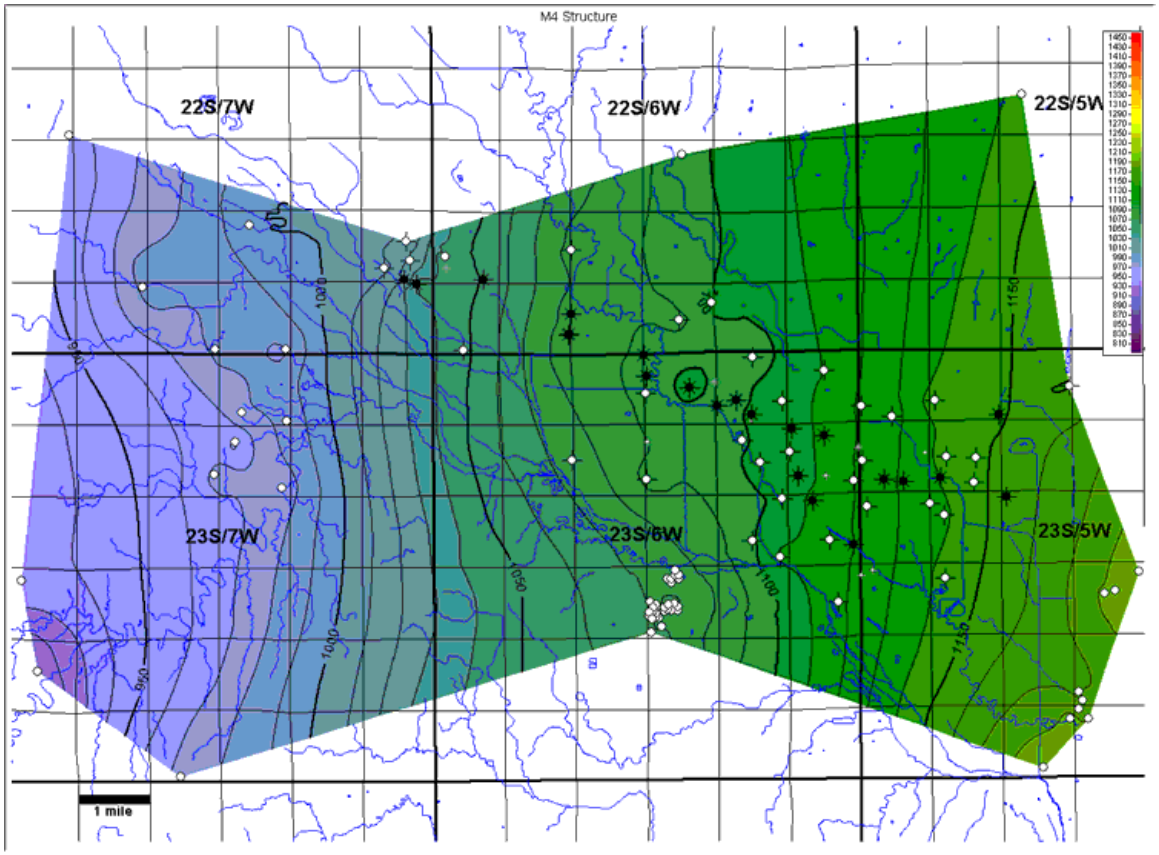

Figure 3E. Structure map of the M4 marker. Contour Interval = 10 ft. Wells within the study area not used in generating this map are displayed in gray at half size.

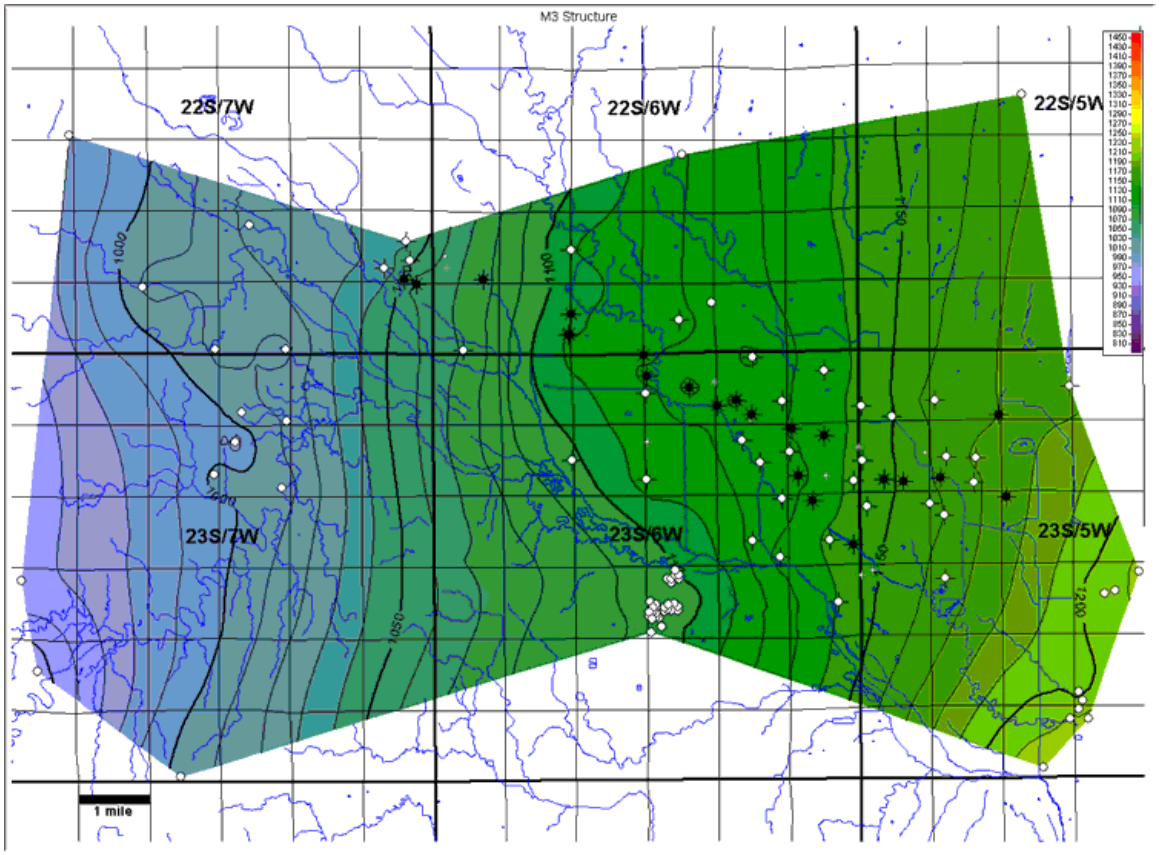

Figure 3F. Structure map of the M3 marker. Contour Interval = 10 ft. Wells within the study area not used in generating this map are displayed in gray at half size.

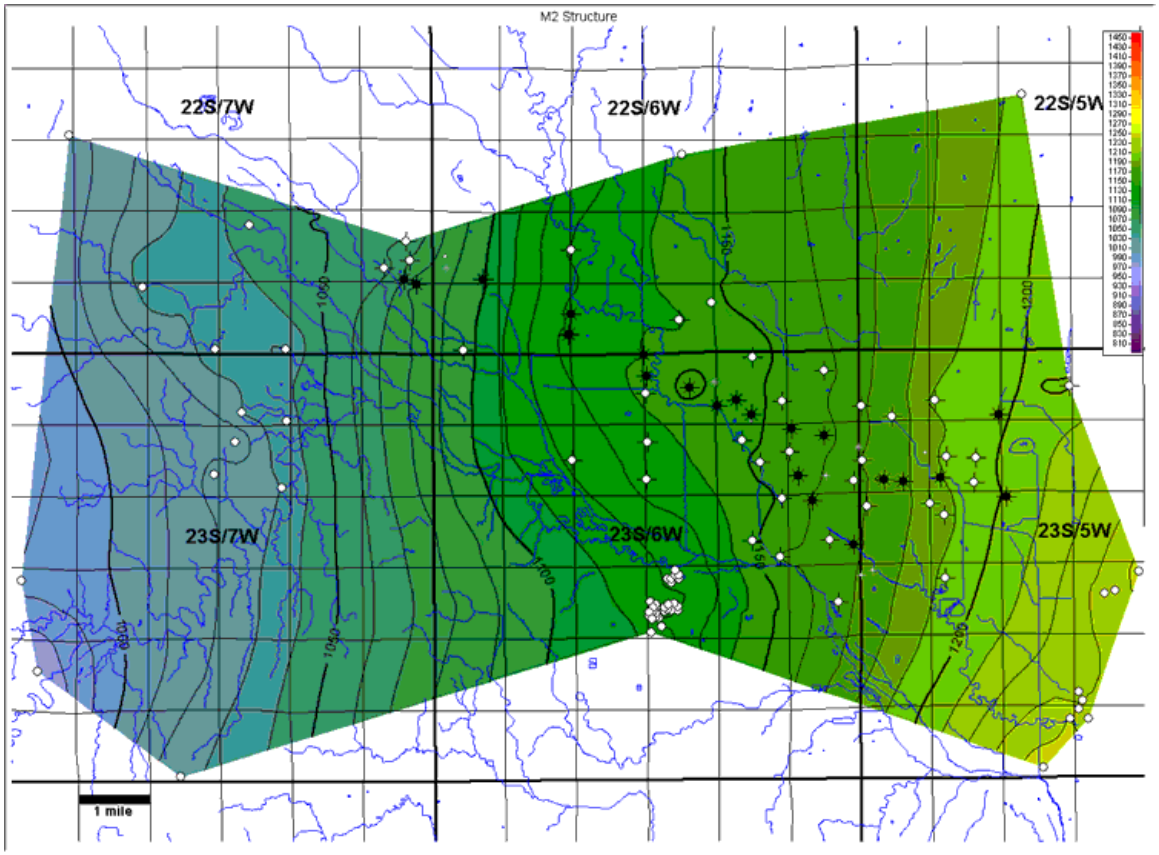

Figure 3G. Structure map of the M2 marker. Contour Interval = 10 ft. Wells within the study area not used in generating this map are displayed in gray at half size.

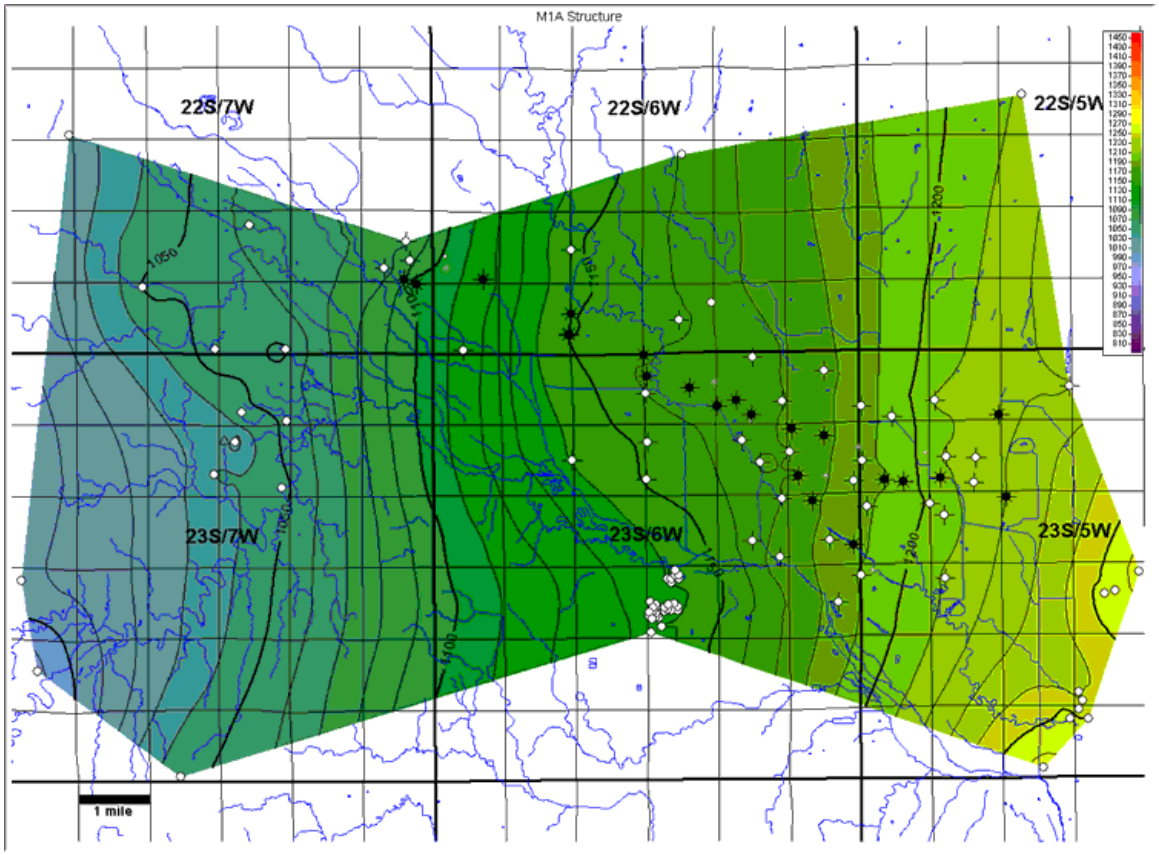

Figure 3H. Structure map of the M1A marker. Contour Interval = 10 ft. Wells within the study area not used in generating this map are displayed in gray at half size.

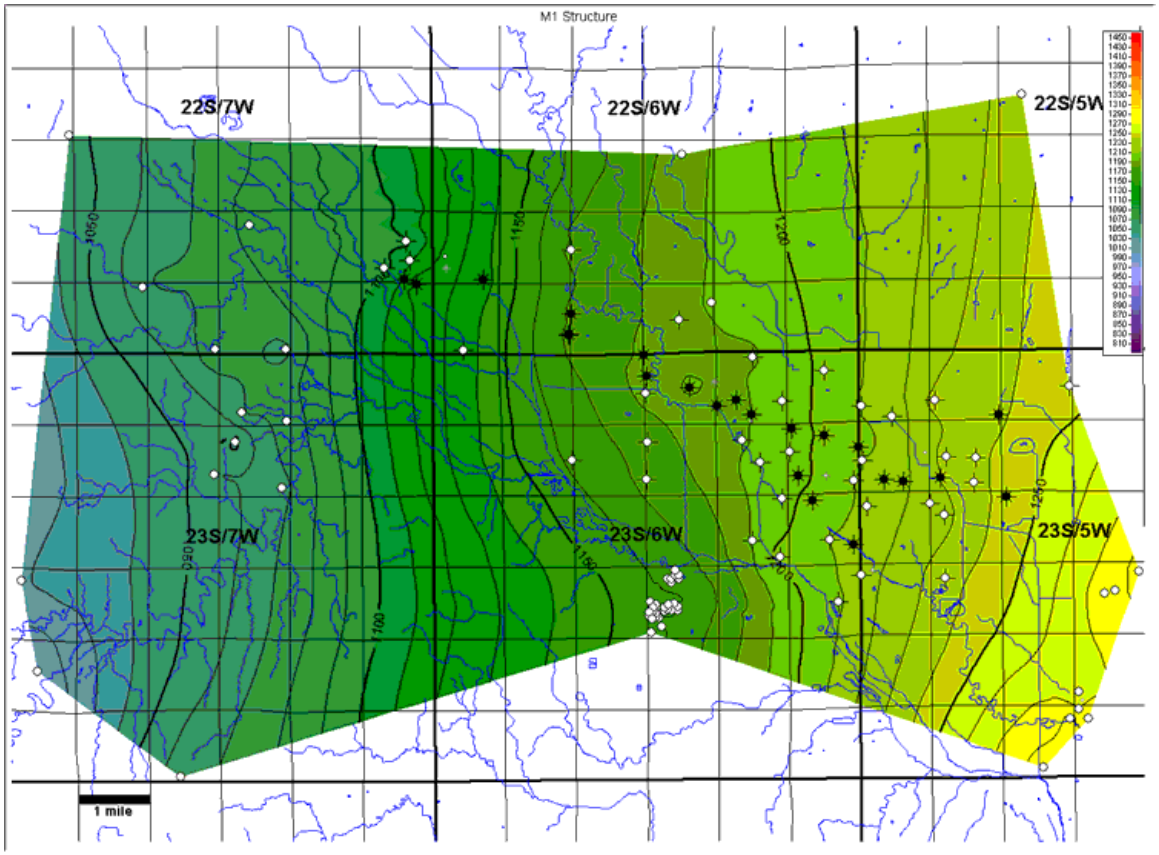

Figure 3I. Structure map of the M1 marker. Contour Interval = 10 ft. Wells within the study area not used in generating this map are displayed in gray at half size.

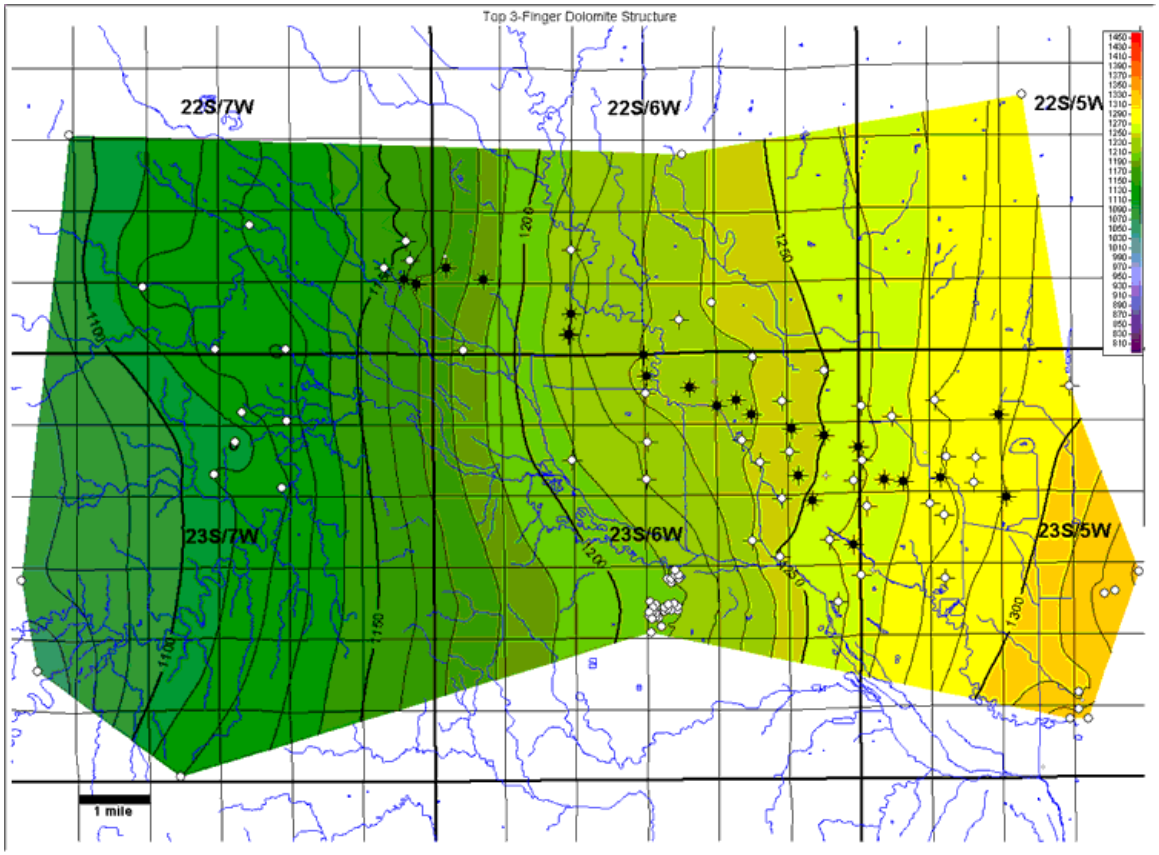

Figure 3J. Structure map of the top 3-finger dolomite. Contour Interval = 10 ft. Wells within the study area not used in generating this map are displayed in gray at half size.

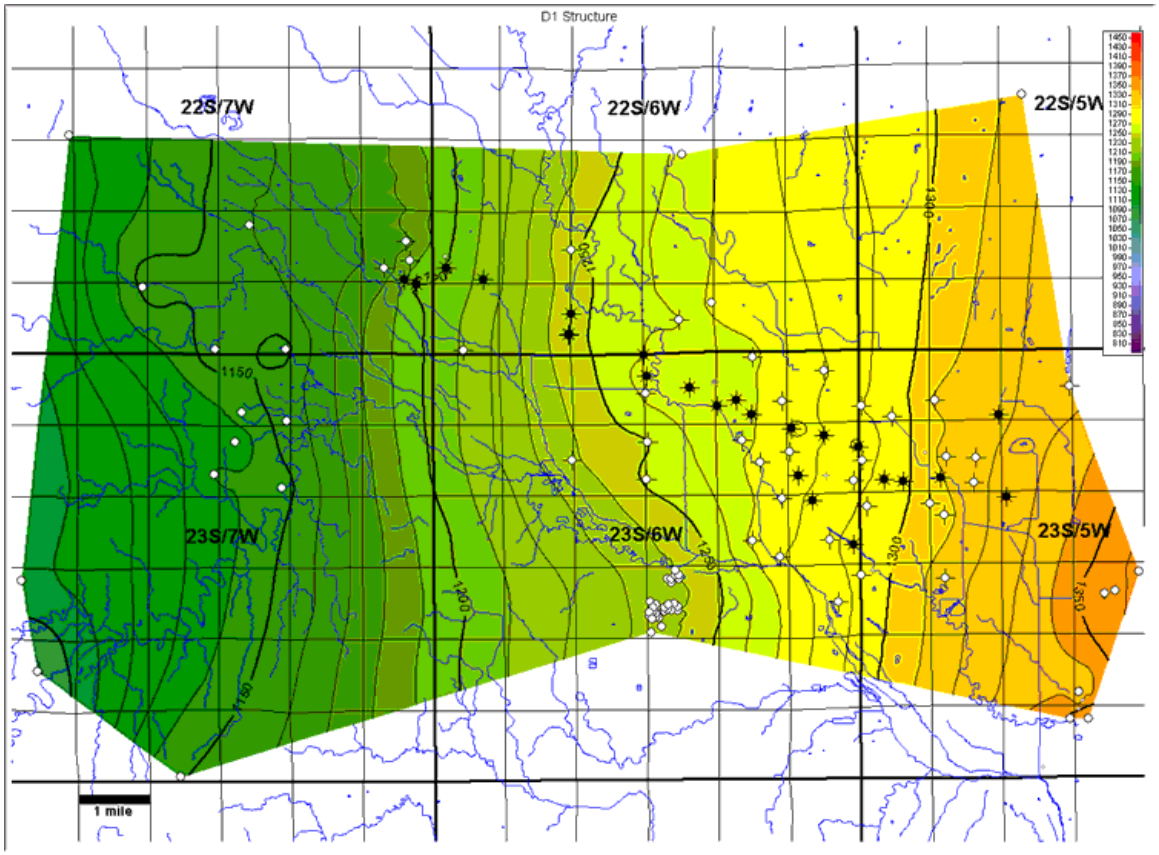

Figure 3K. Structure map of the D1 marker. Contour Interval = 10 ft. Wells within the study area not used in generating this map are displayed in gray at half size.

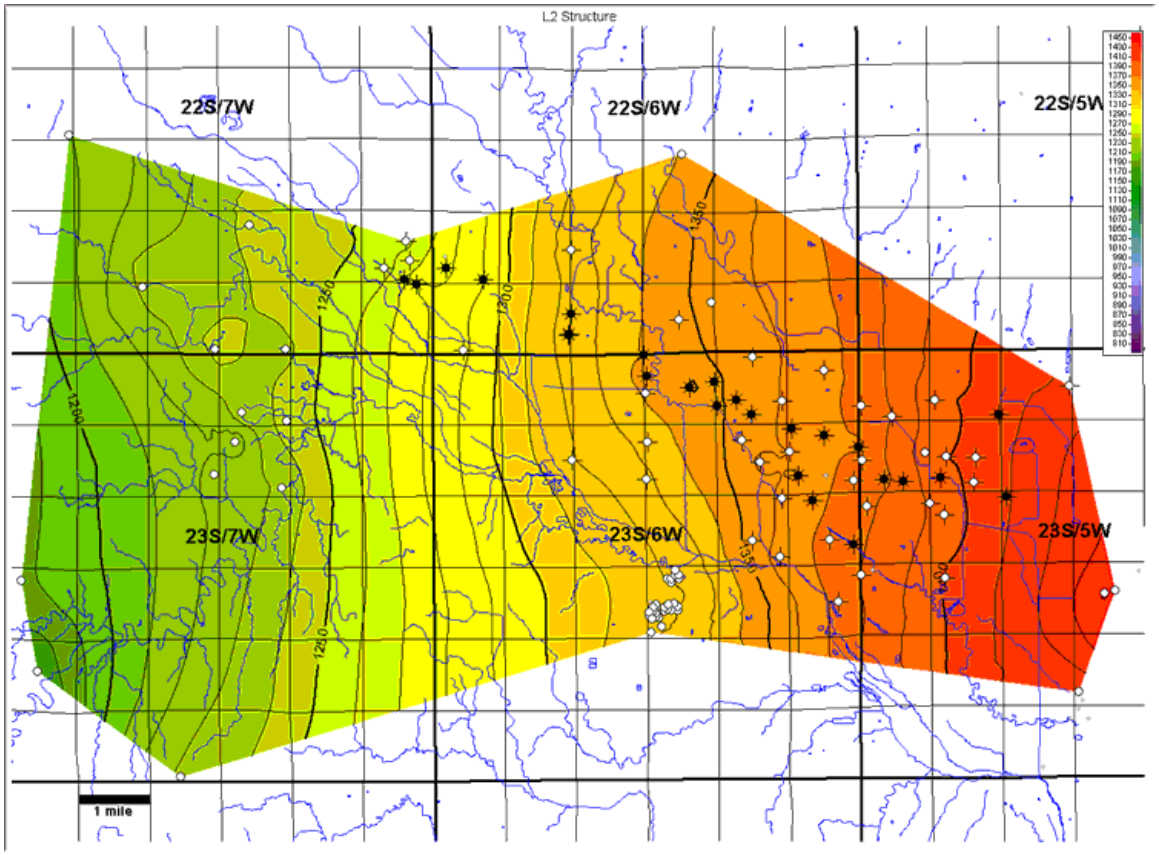

Figure 3L. Structure map of the L2 marker. Contour Interval = 10 ft. Wells within the study area not used in generating this map are displayed in gray at half size.

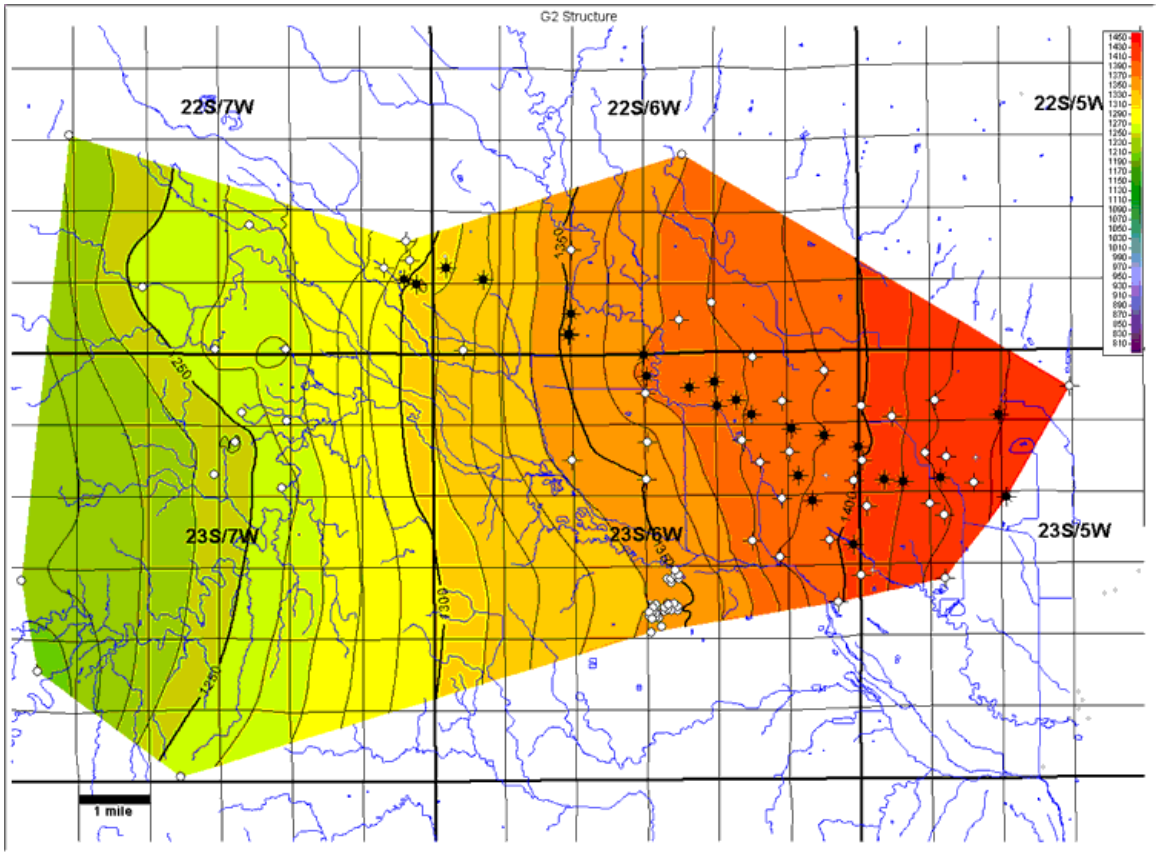

Figure 3M. Structure map of the G2 marker. Contour Interval = 10 ft. Wells within the study area not used in generating this map are displayed in gray at half size.

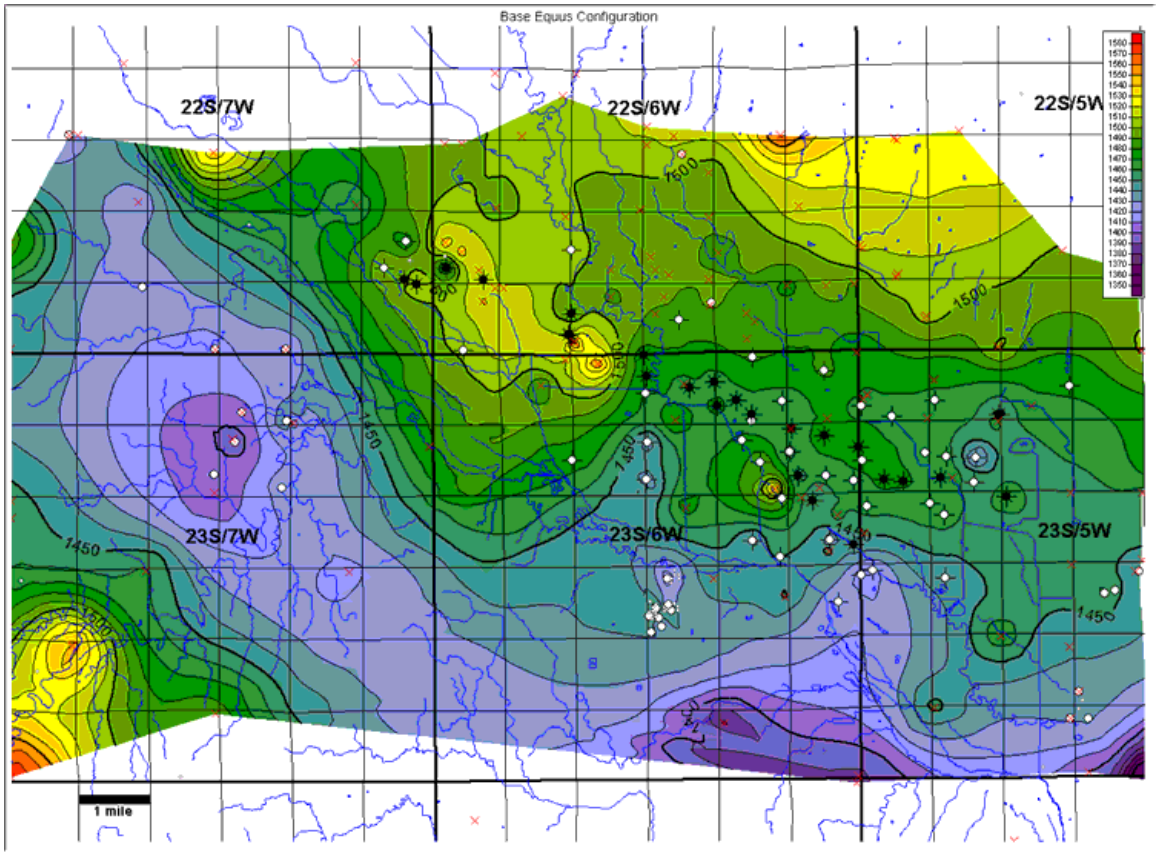

Figure 3N. Configuration map of the Base of Quaternary Equus Beds. Contour Interval = 10 ft. Wells within the study area not used in generating this map are displayed in gray at half size. Red crosses indicate supplemental control points from water well completion records, test holes, and KGS publications, which have been used in mapping the Base Equus configuration.

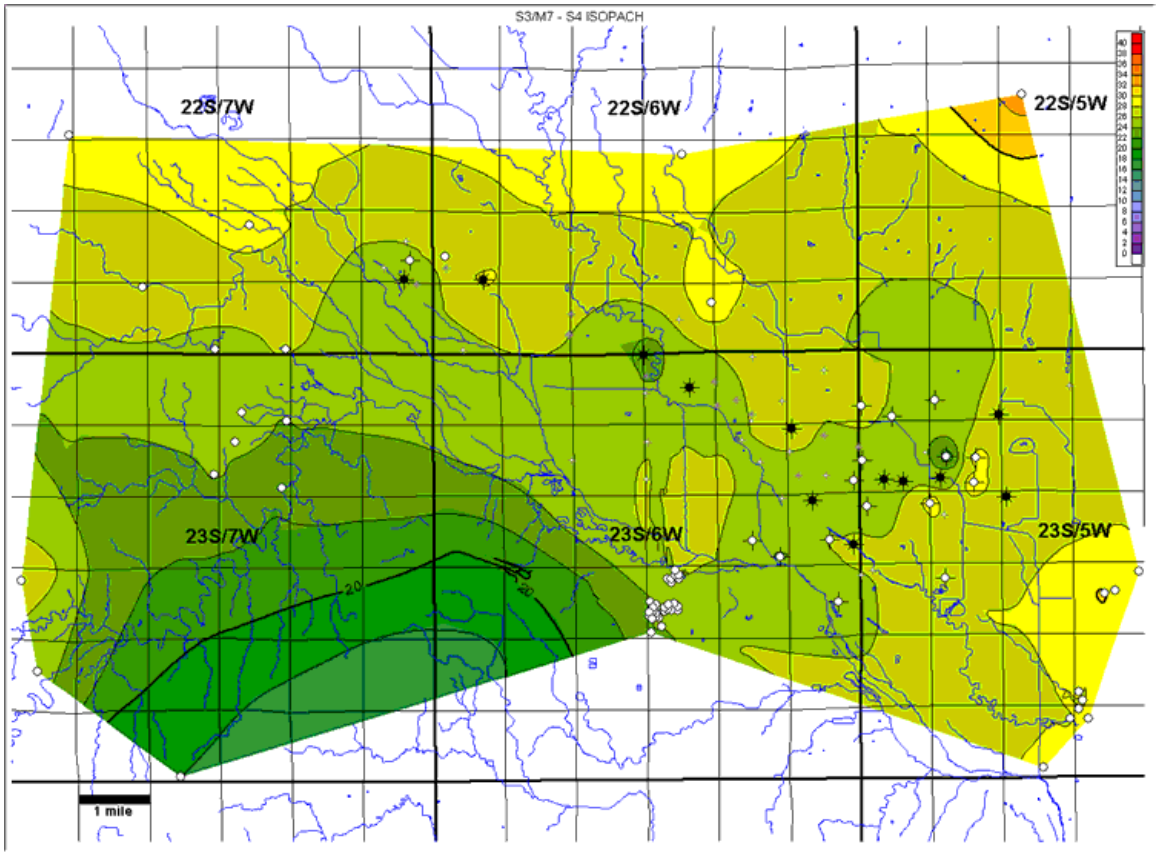

Figure 4A. Isopach map of the interval between markers S3/M7 and S4. Contour interval = 2 ft. Wells within the study area not used in generating this map are displayed in gray at half size.

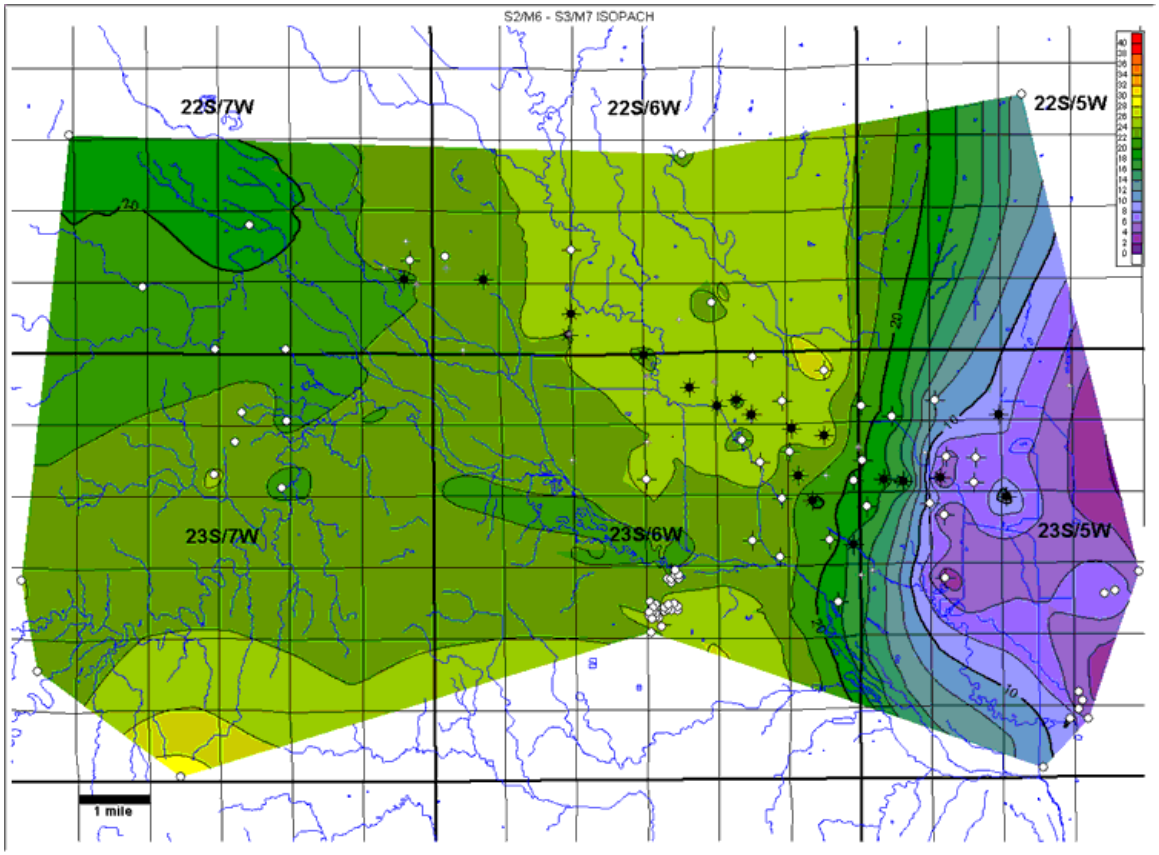

Figure 4B. Isopach map of the interval between markers S2/M6 and S3/M7. Contour interval = 2 ft. Wells within the study area not used in generating this map are displayed in gray at half size.

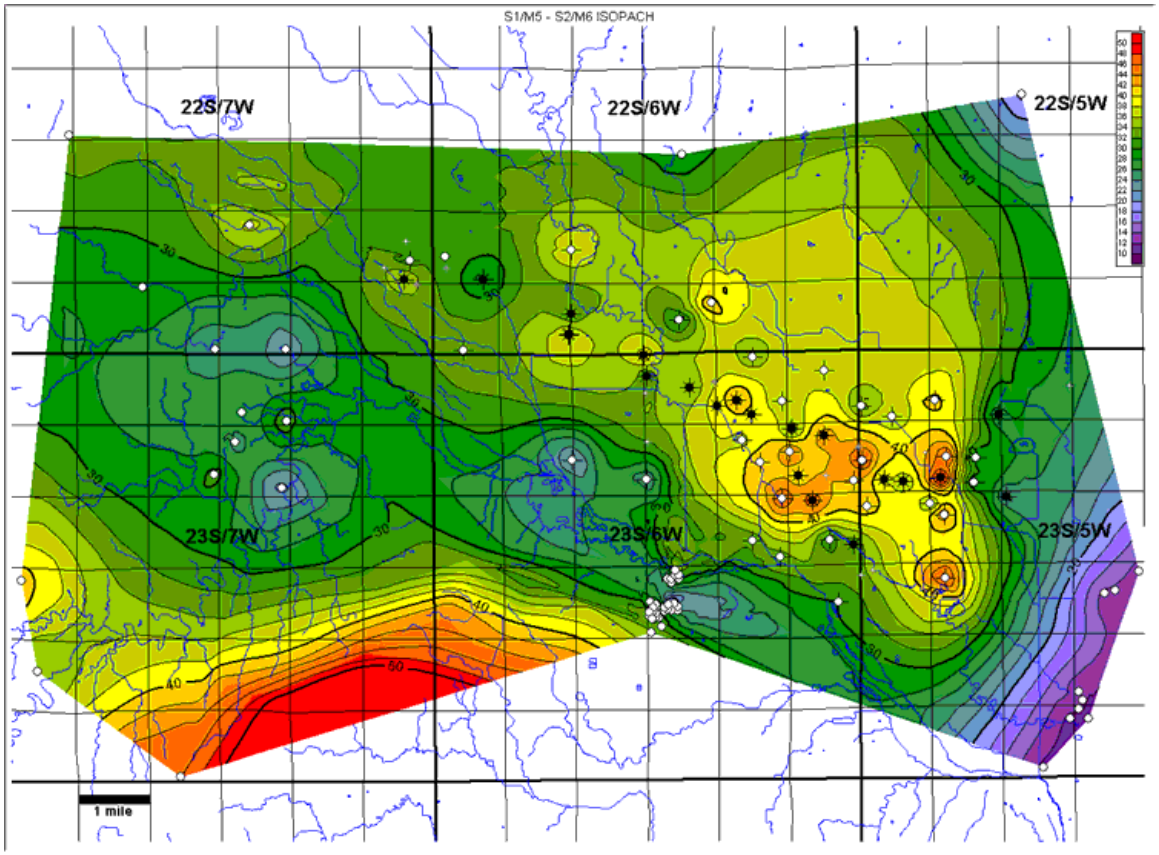

Figure 4C. Isopach map of the interval between markers S1/M5 and S2/M6. Contour interval = 2 ft. Wells within the study area not used in generating this map are displayed in gray at half size.

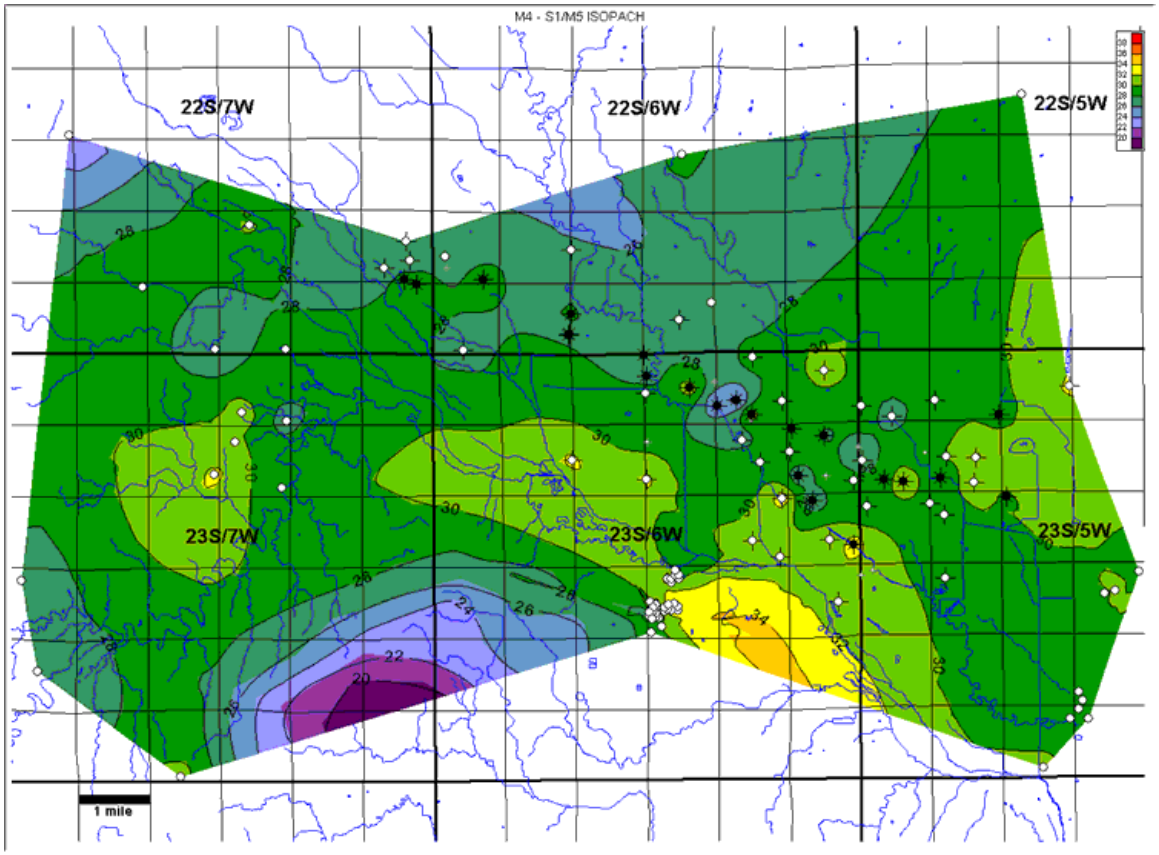

Figure 4D. Isopach map of the interval between markers M4 and S1/M5. Contour interval = 2 ft. Wells within the study area not used in generating this map are displayed in gray at half size.

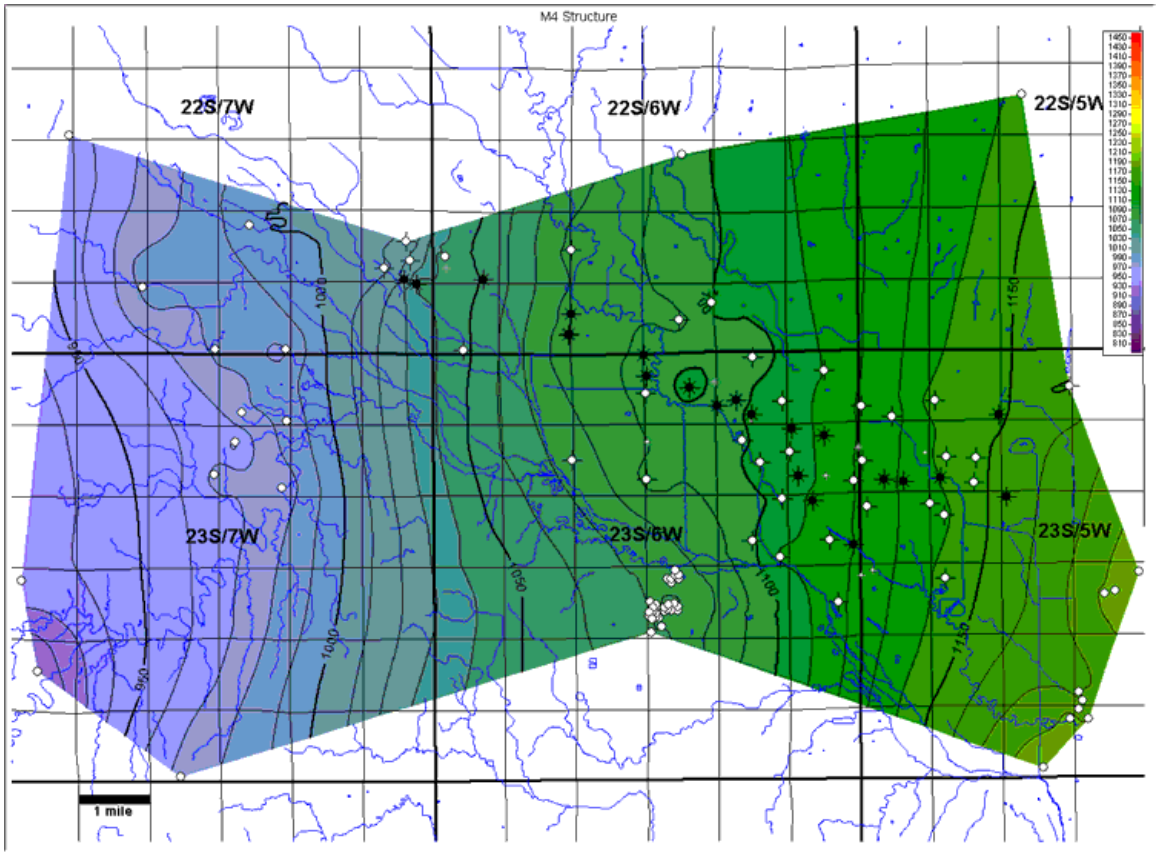

Figure 4E. Isopach map of the interval between markers M3 and M4. Contour interval = 2 ft. Wells within the study area not used in generating this map are displayed in gray at half size.

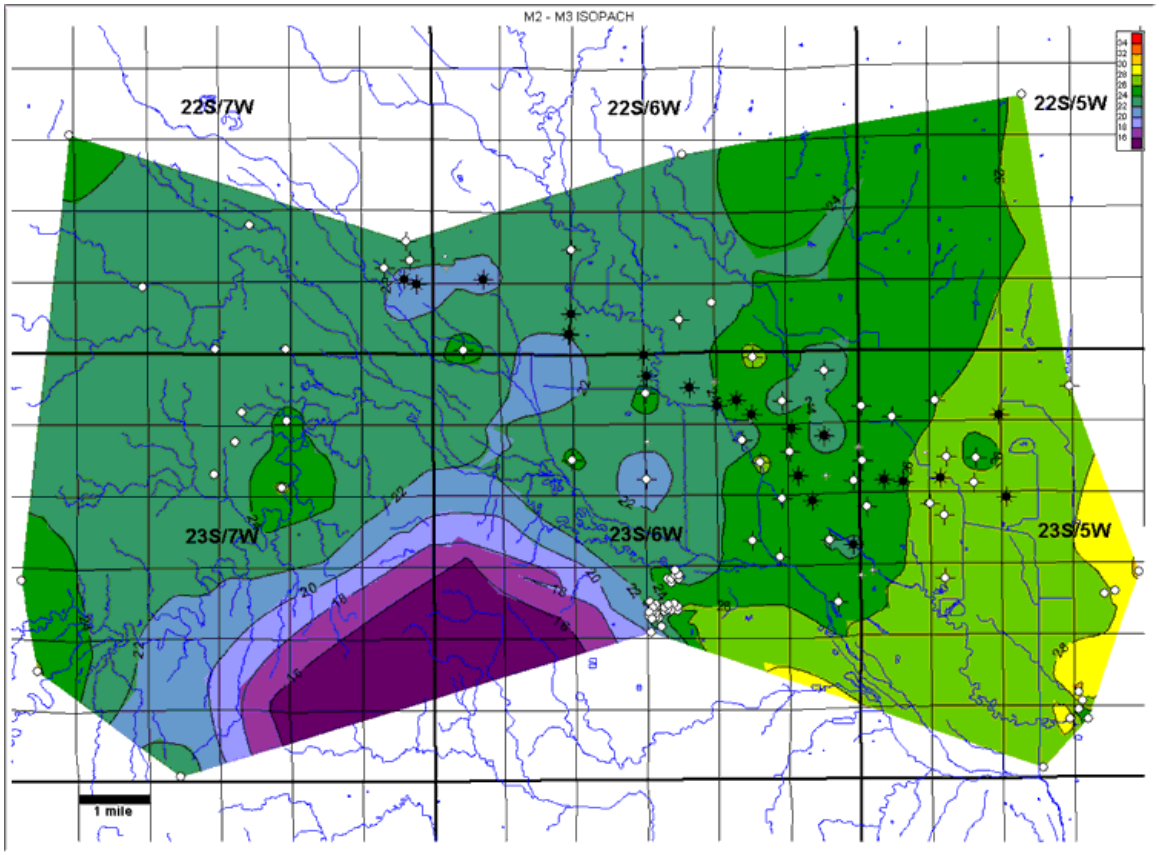

Figure 4F. Isopach map of the interval between markers M2 and M3. Contour interval = 2 ft. Wells within the study area not used in generating this map are displayed in gray at half size.

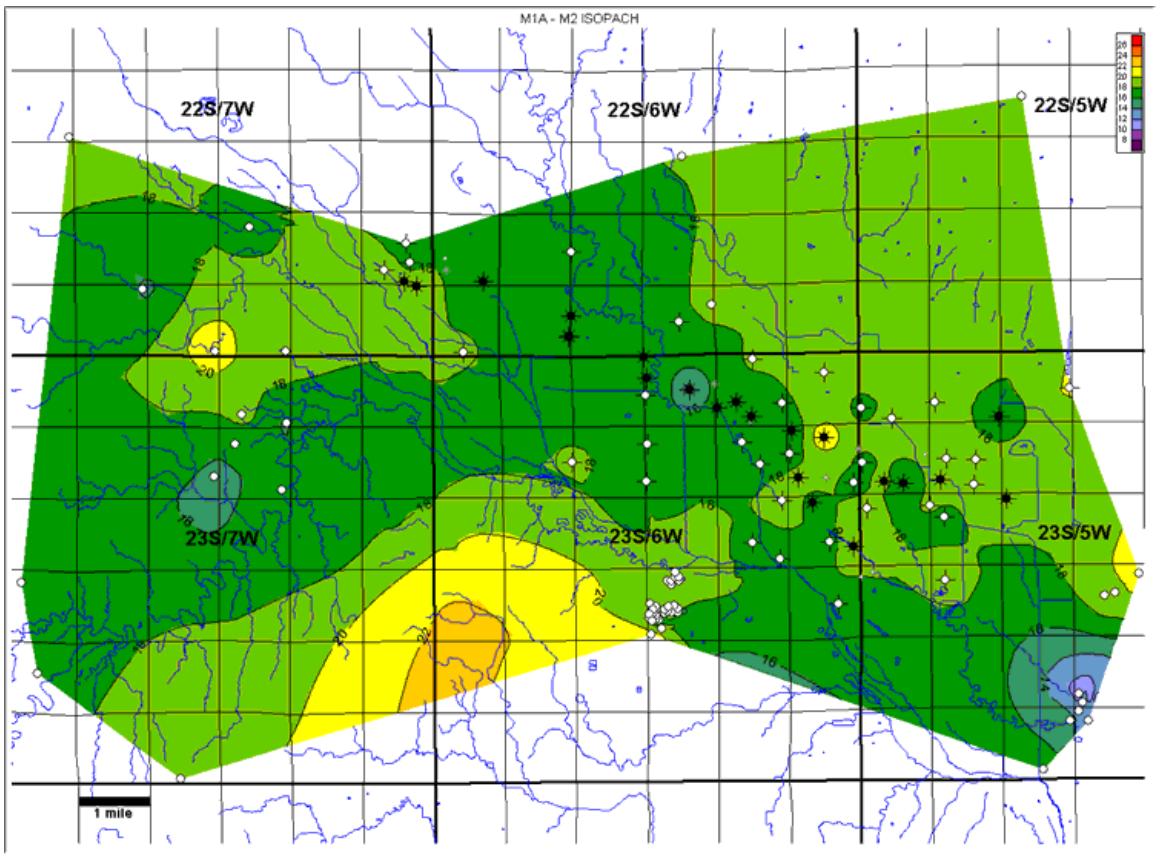

Figure 4G. Isopach map of the interval between markers M1A and M2. Contour interval = 2 ft. Wells within the study area not used in generating this map are displayed in gray at half size.

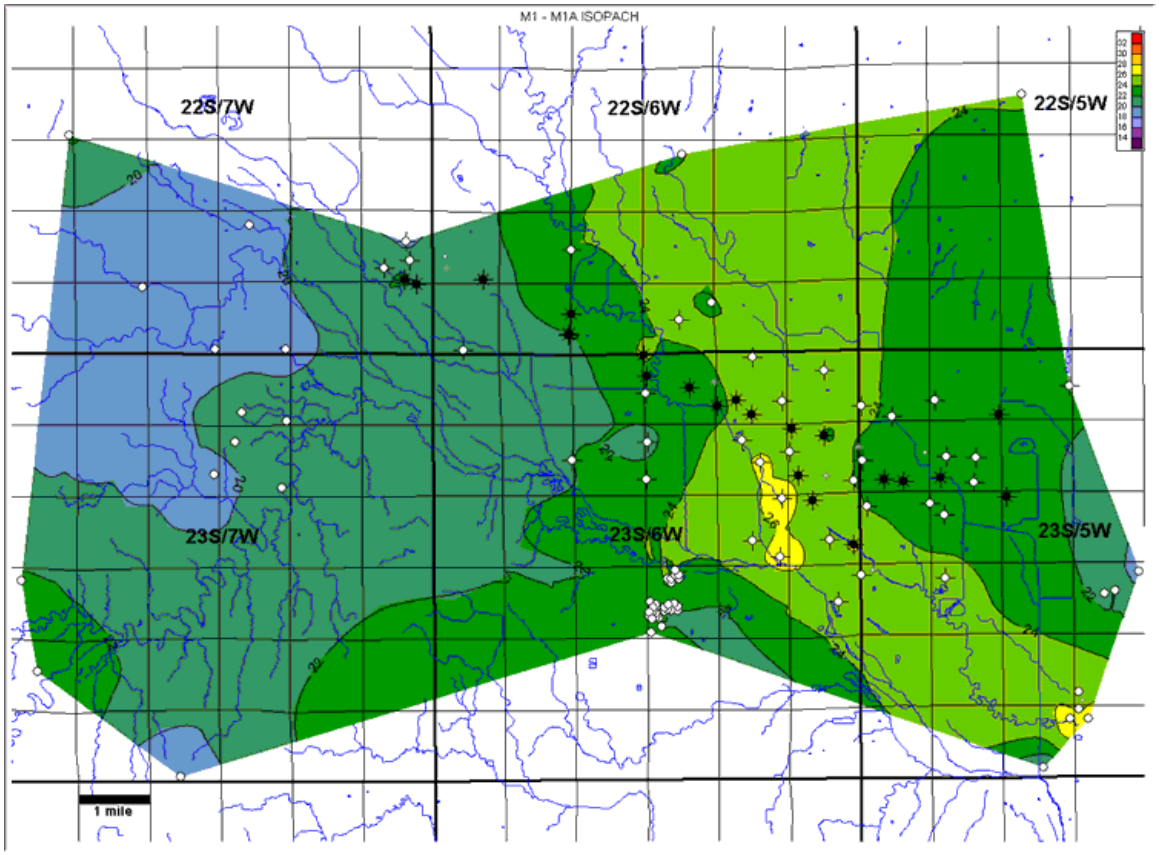

Figure 4H. Isopach map of the interval between markers M1 and M1A. Contour interval = 2 ft. Wells within the study area not used in generating this map are displayed in gray at half size.

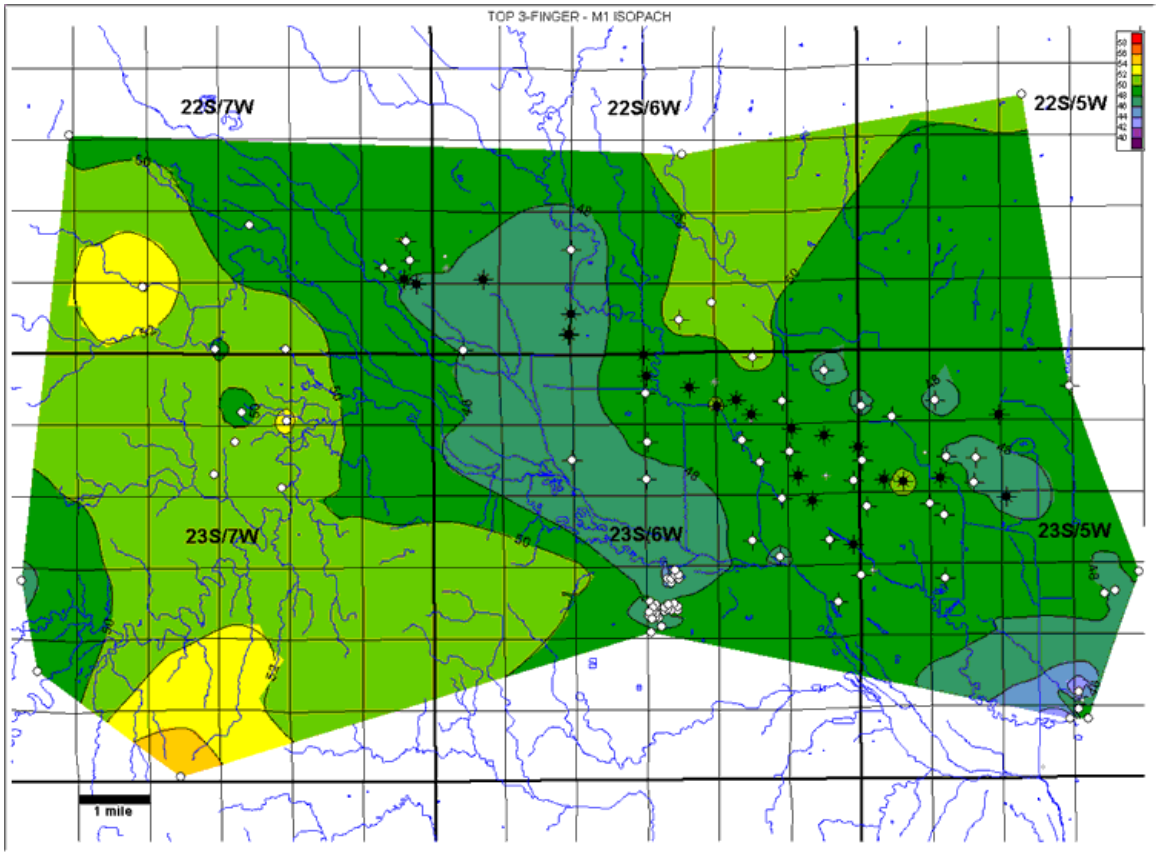

Figure 4I. Isopach map of the interval between the top 3-finger dolomite and marker M1. Contour interval = 2 ft. Wells within the study area not used in generating this map are displayed in gray at half size.

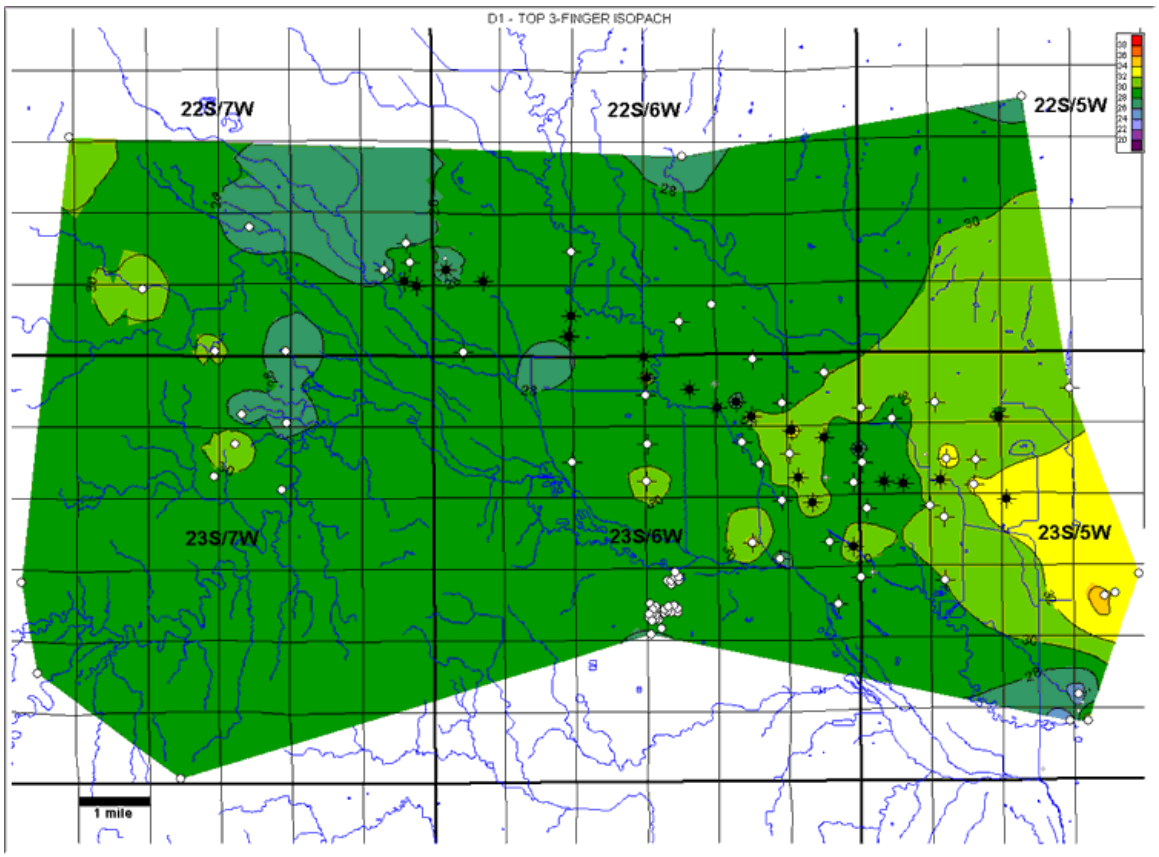

Figure 4J. Isopach map of the interval between marker D1 and the top 3-finger dolomite. Contour interval = 2 ft. Wells within the study area not used in generating this map are displayed in gray at half size.

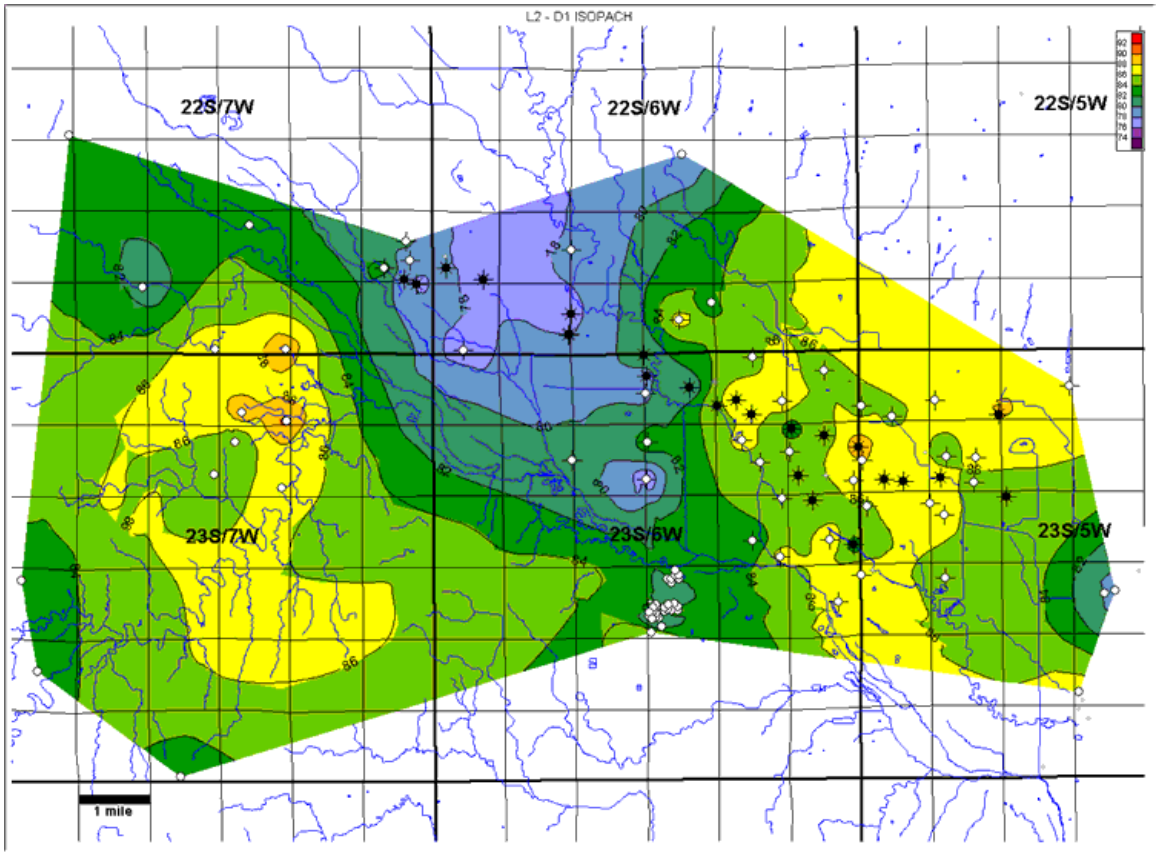

Figure 4K. Isopach map of the interval between markers L2 and D1. Contour interval = 2 ft. Wells within the study area not used in generating this map are displayed in gray at half size.

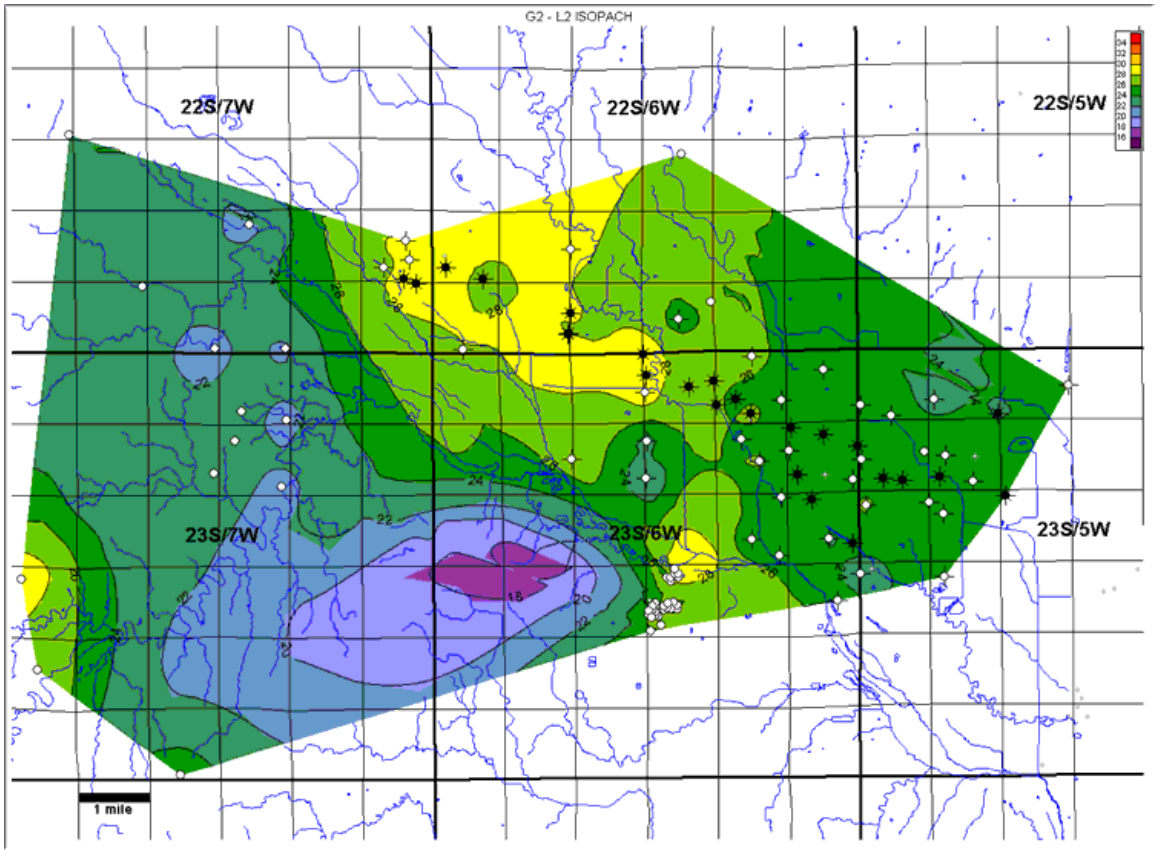

Figure 4L. Isopach map of the interval between markers G2 and L2. Contour interval = 2 ft. Wells within the study area not used in generating this map are displayed in gray at half size.

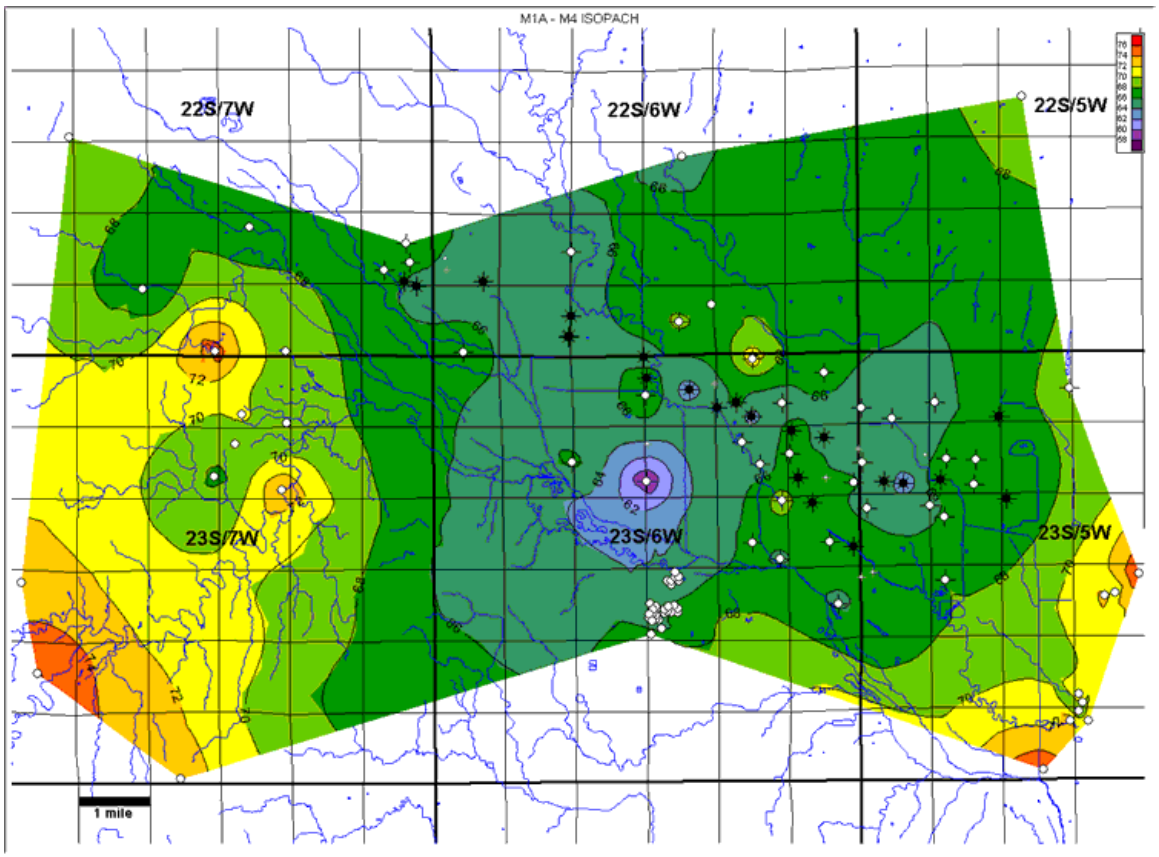

Figure 5A. Isopach map of the interval between markers M1A and M4. Contour interval = 2 ft. Wells within the study area not used in generating this map are displayed in gray at half size.

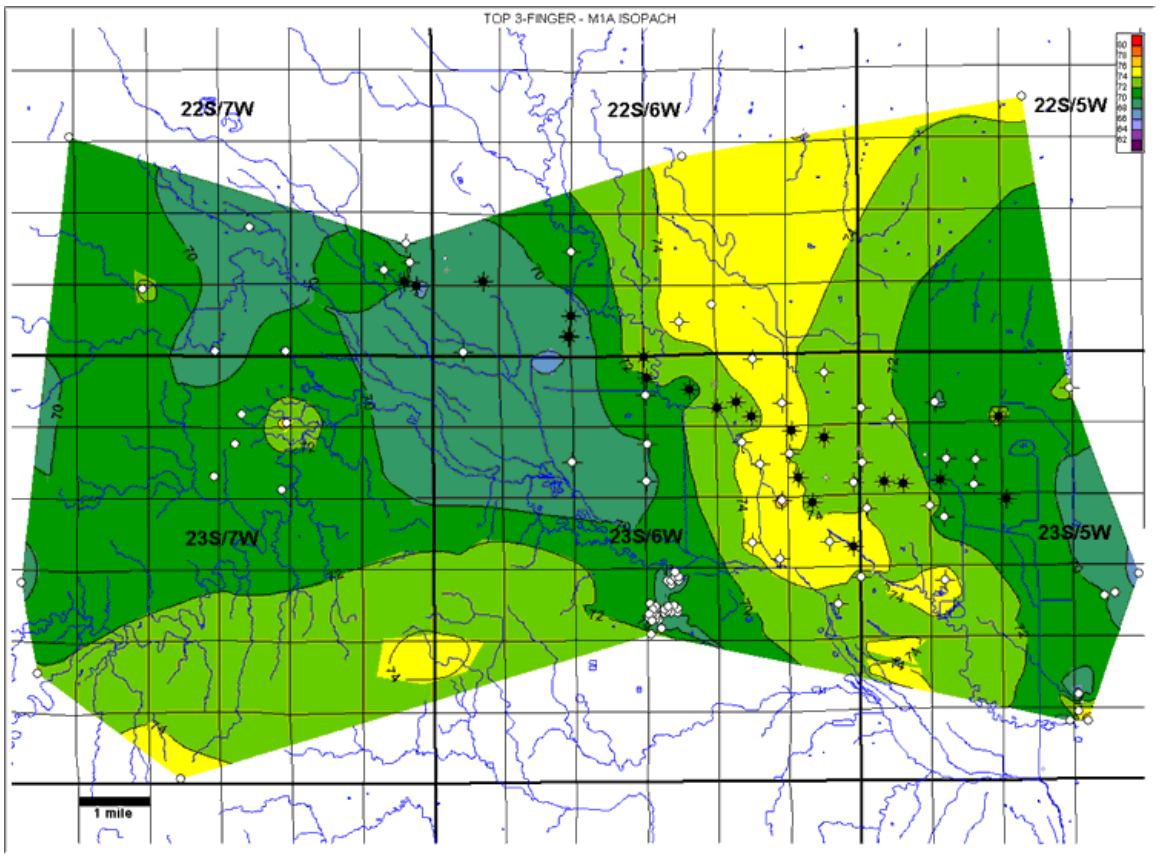

Figure 5B. Isopach map of the interval between the top 3-finger dolomite and marker M1A. Contour interval = 2 ft. Wells within the study area not used in generating this map are displayed in gray at half size.

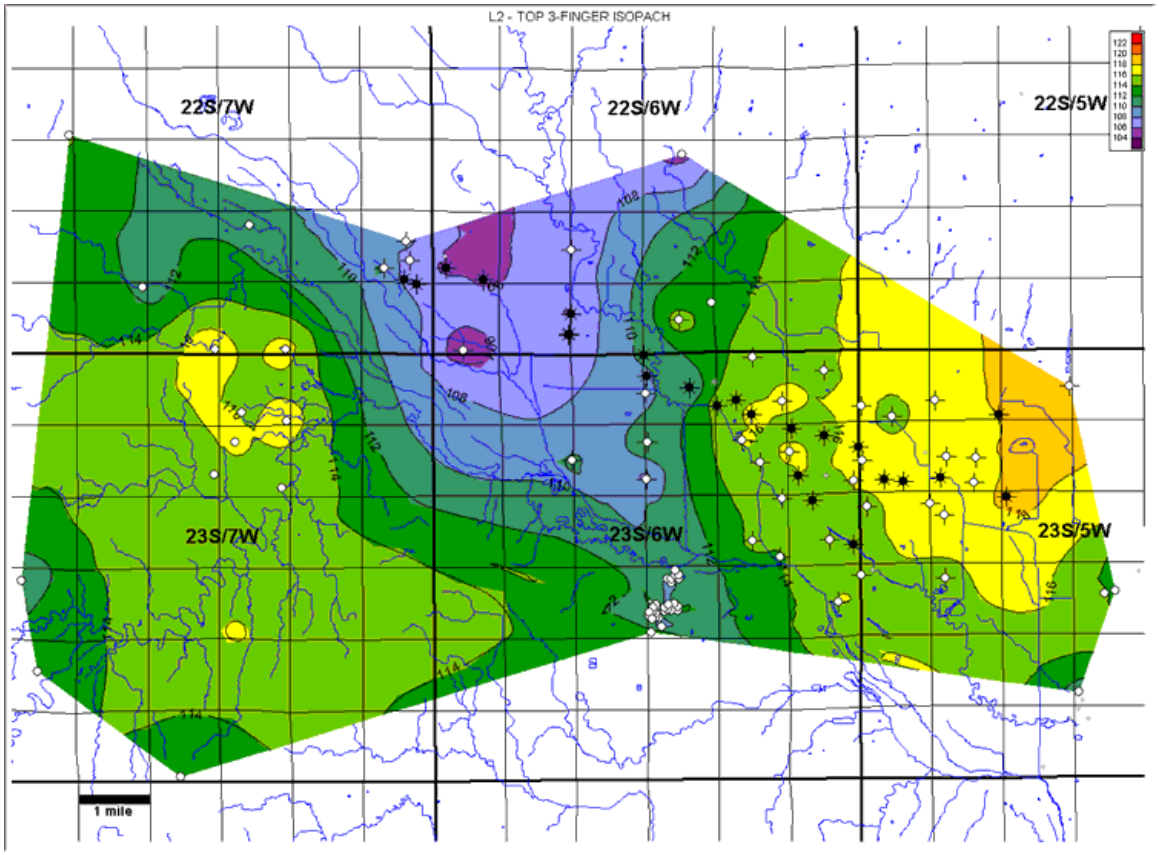

Figure 5C. Isopach map of the interval between marker L2 and the top 3-finger dolomite. Contour interval = 2 ft. Wells within the study area not used in generating this map are displayed in gray at half size.

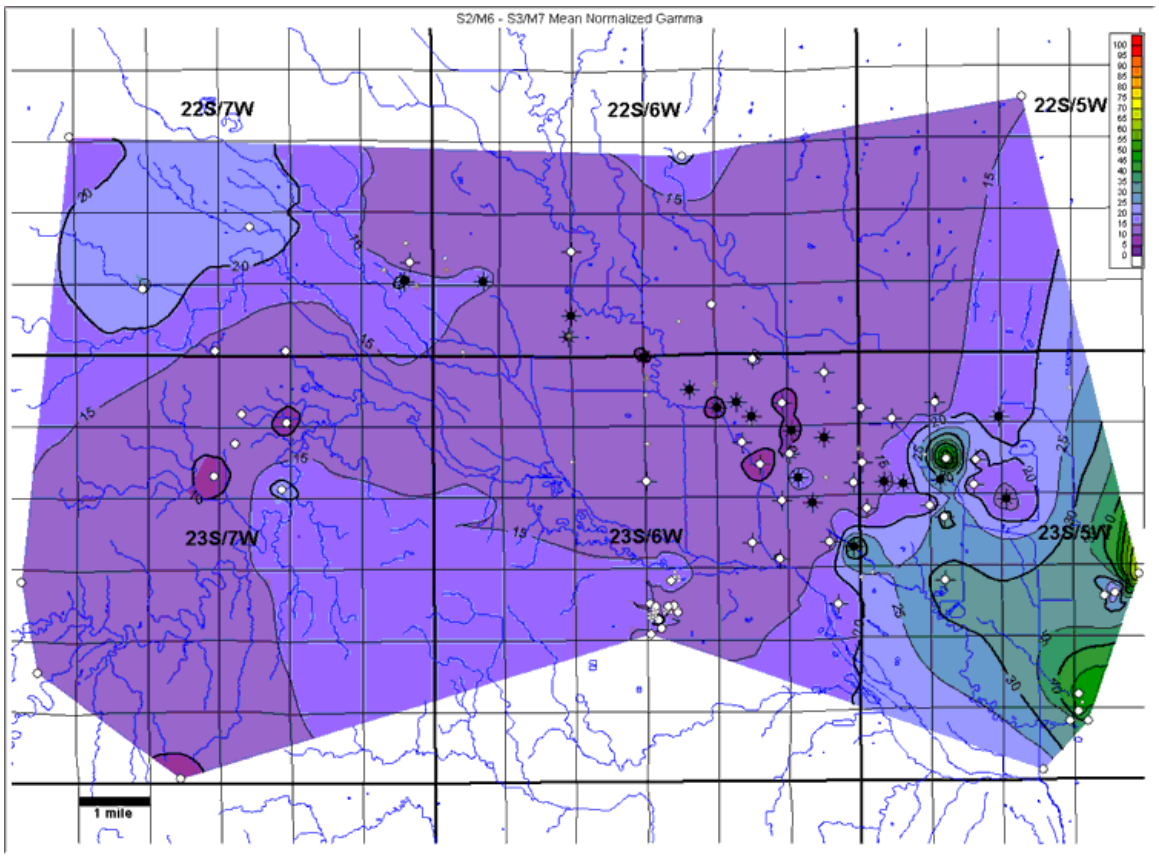

Figure 6A. Mean normalized natural-gamma ray for the S2/M6 – S3/M7 interval, showing the facies change at the eastern edge of the study area. Values are % shale. Contour interval = 5%. Wells within the study area not used in generating this map are displayed in gray at half size.

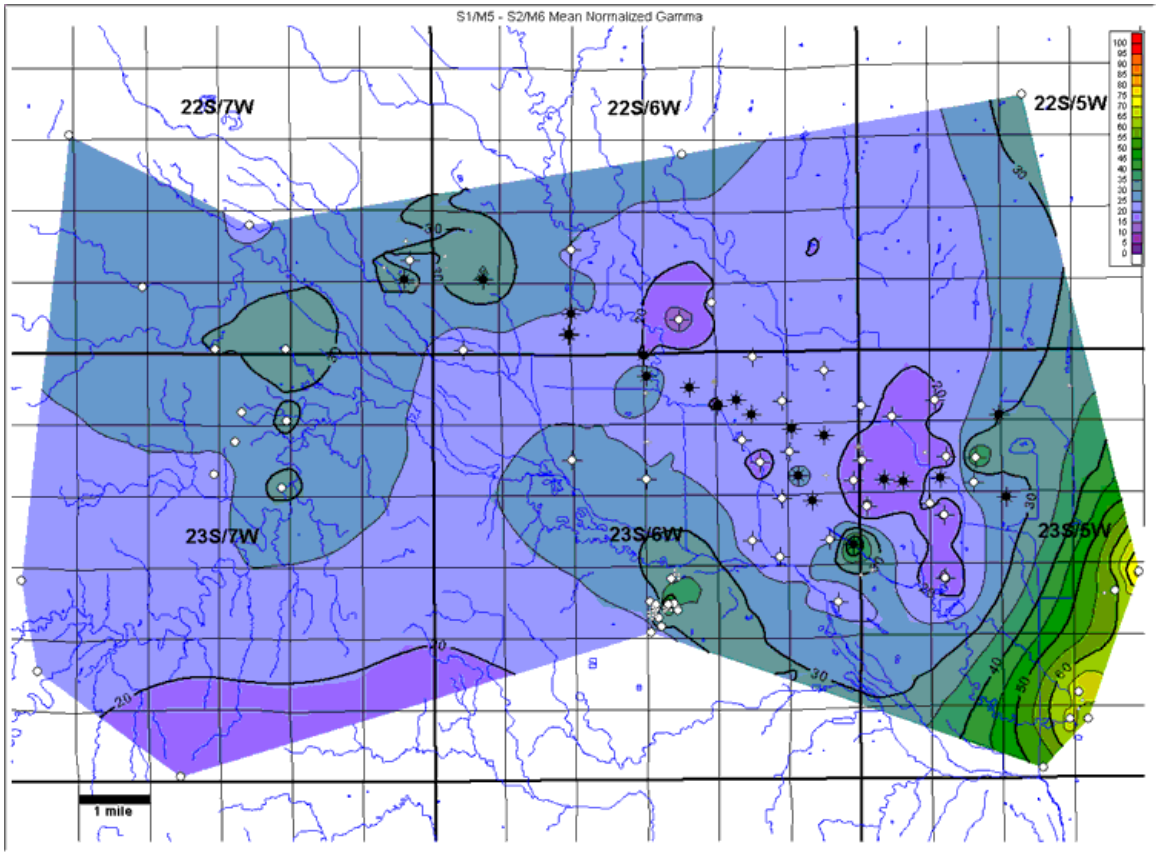

Figure 6B. Mean normalized natural-gamma ray for the S1/M5 – S2/M6 interval, showing the facies change at the eastern edge of the study area. Values are % shale. Contour interval = 5%. Wells within the study area not used in generating this map are displayed in gray at half size.

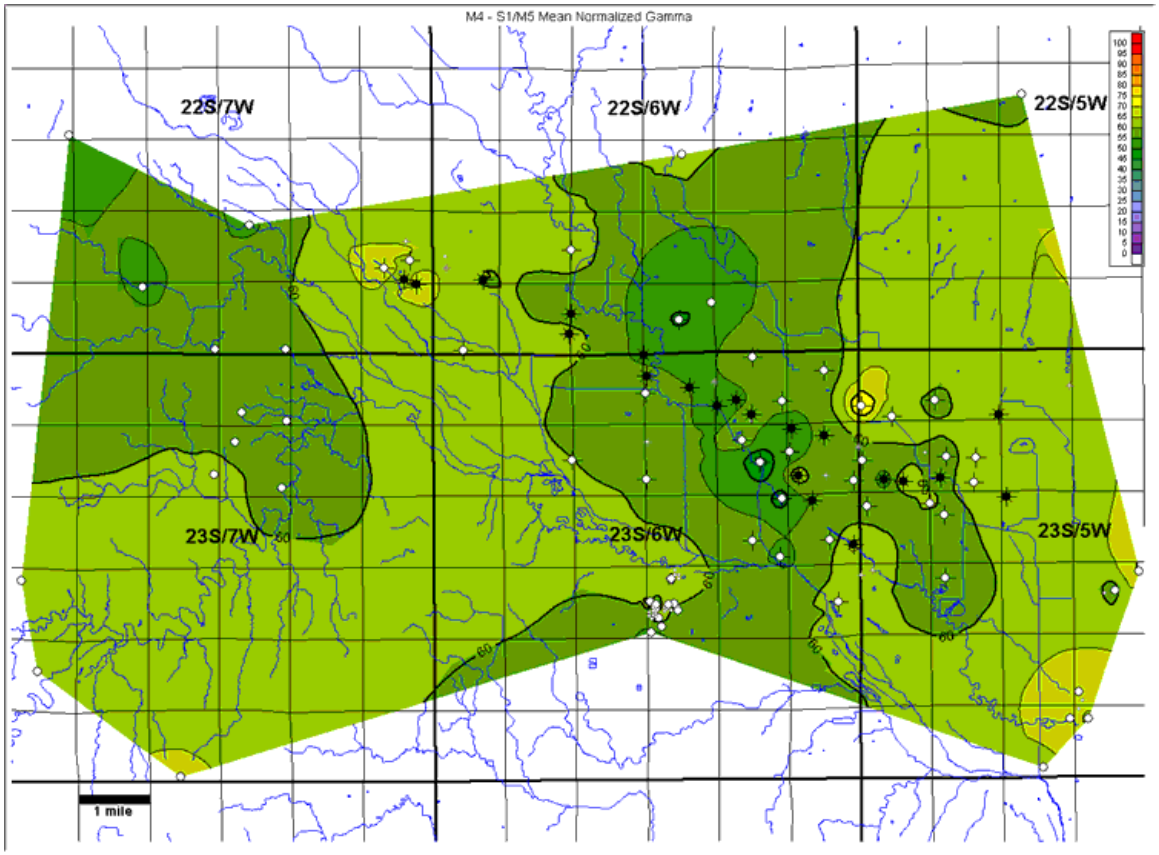

Figure 6C. Mean normalized natural-gamma ray for the M4–S1/M5 interval. Values are % shale. Contour interval = 5%. Wells within the study area not used in generating this map are displayed in gray at half size.

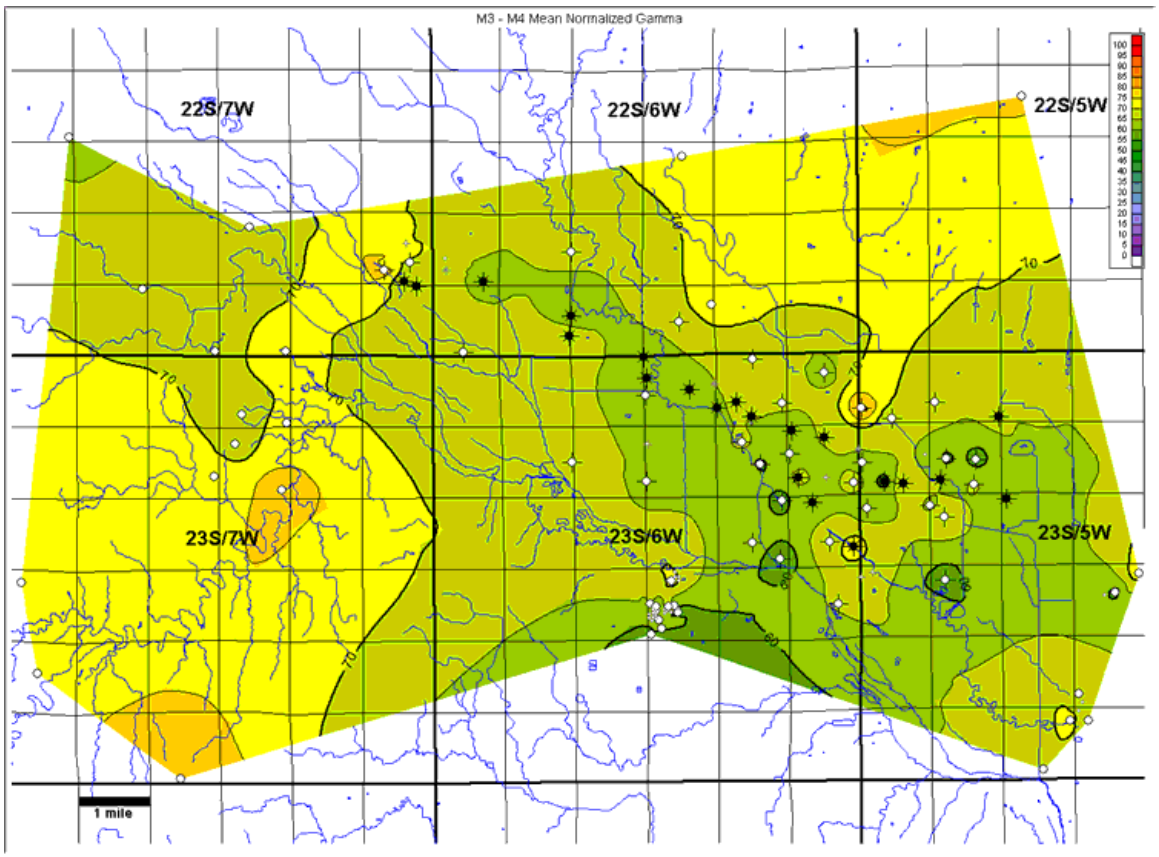

Figure 6D. Mean normalized natural-gamma ray for the M3-M4 interval. Values are % shale. Contour interval = 5%. Wells within the study area not used in generating this map are displayed in gray at half size.

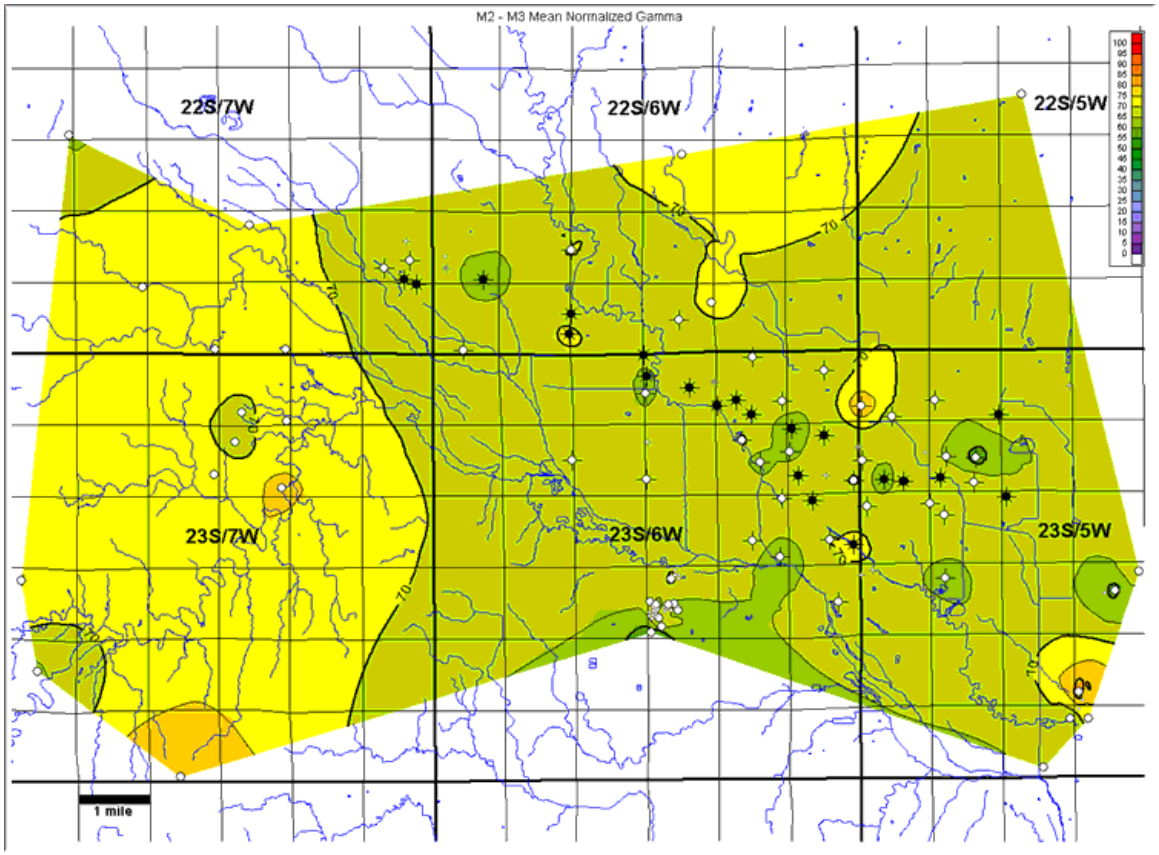

Figure 6E. Mean normalized natural-gamma ray for the M2-M3 interval. Values are % shale. Contour interval = 5%. Wells within the study area not used in generating this map are displayed in gray at half size.

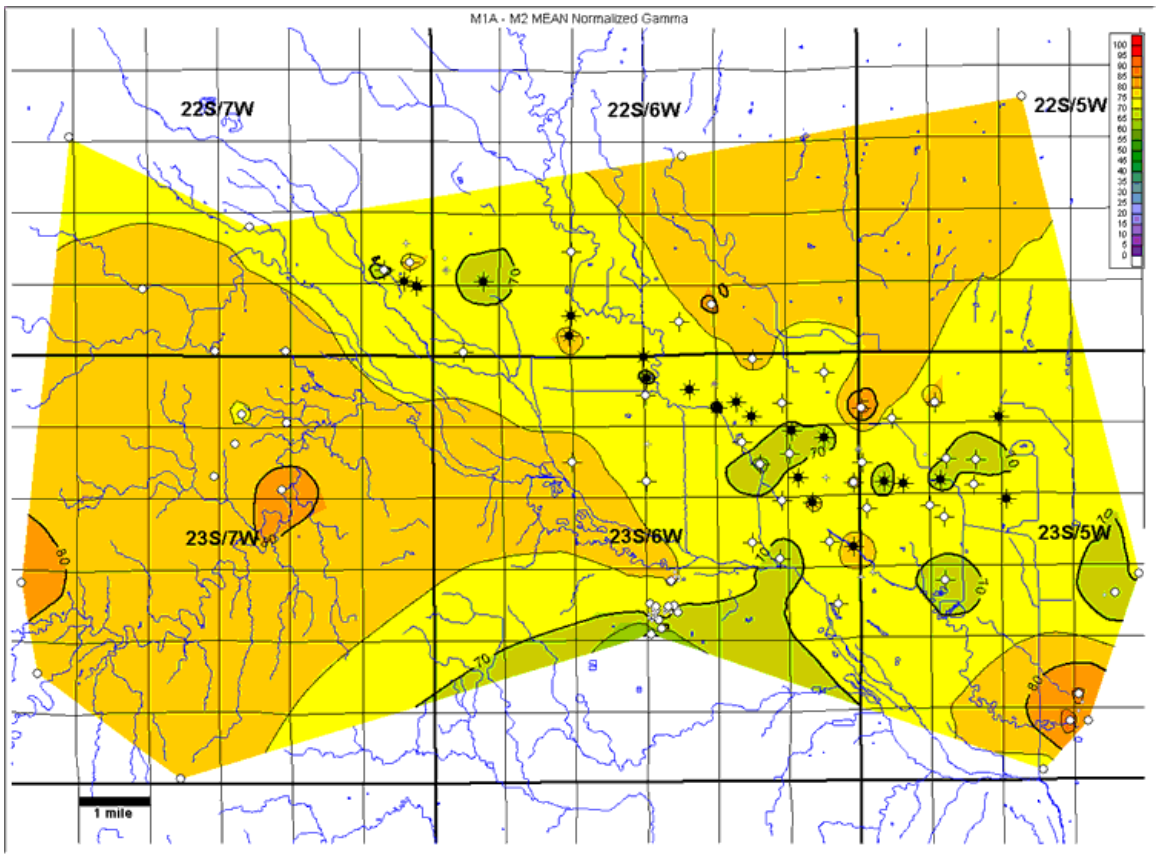

Figure 6F. Mean normalized natural-gamma ray for the M1A-M2 interval. Values are % shale. Contour interval = 5%. Wells within the study area not used in generating this map are displayed in gray at half size.

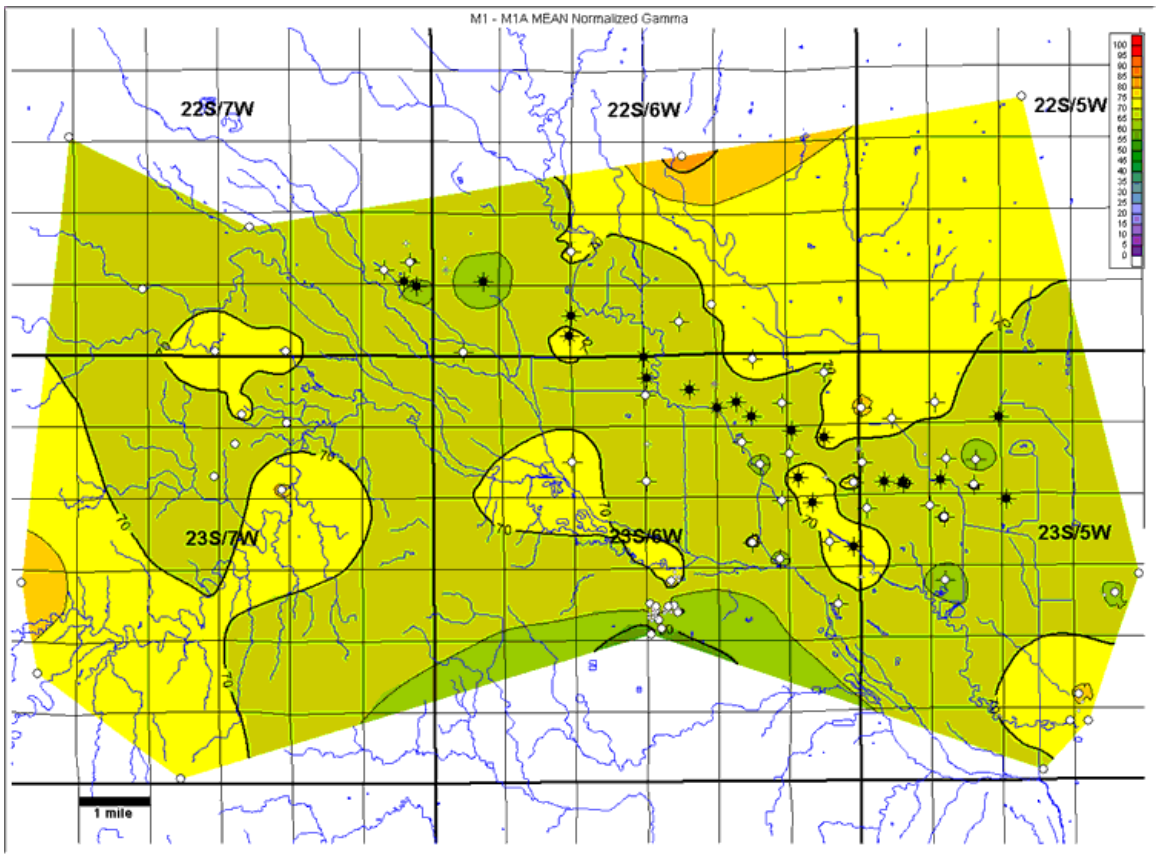

Figure 6G. Mean normalized natural-gamma ray for the M1-M1A interval. Values are % shale. Contour interval = 5%. Wells within the study area not used in generating this map are displayed in gray at half size.

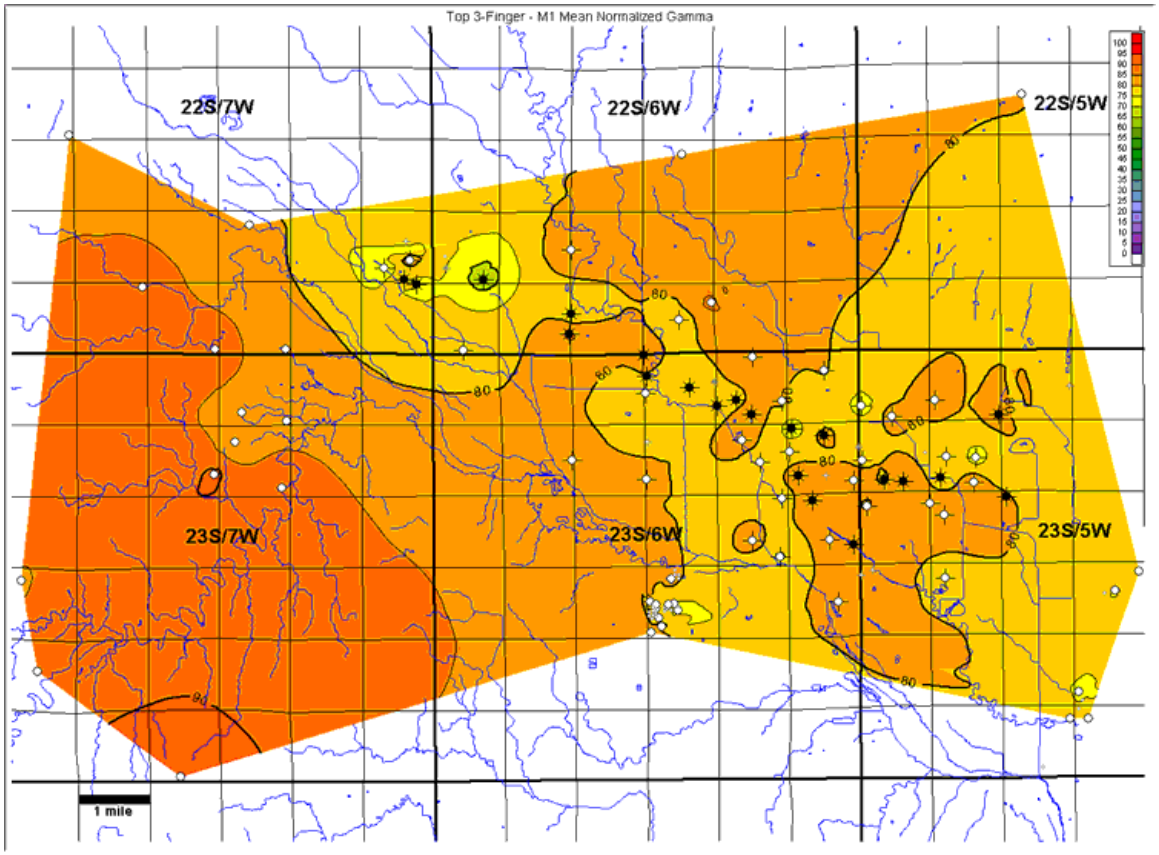

Figure 6H. Mean normalized natural-gamma ray for the Top 3-finger dolomite-M1 interval. Values are % shale. Contour interval = 5%. Wells within the study area not used in generating this map are displayed in gray at half size.

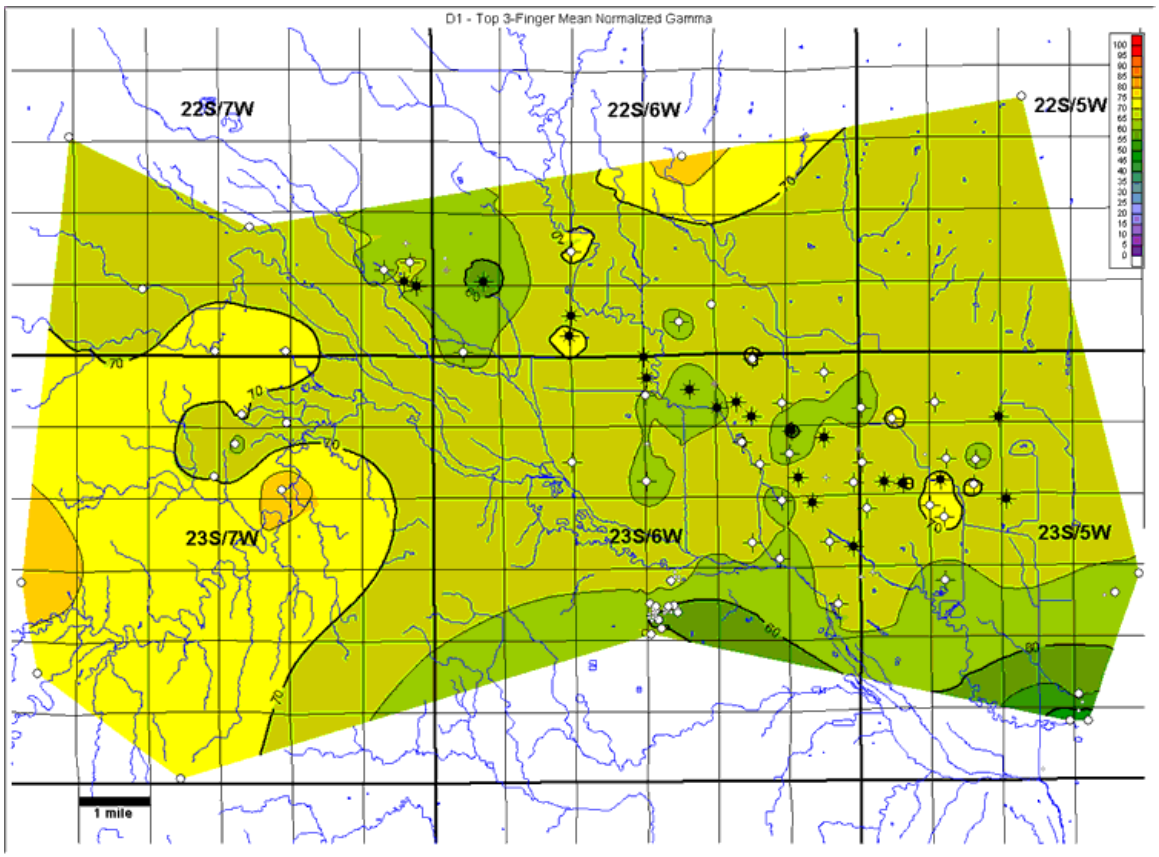

Figure 6I. Mean normalized natural-gamma ray for the D1-Top 3-finger dolomite interval. Values are % shale. Contour interval = 5%. Wells within the study area not used in generating this map are displayed in gray at half size.

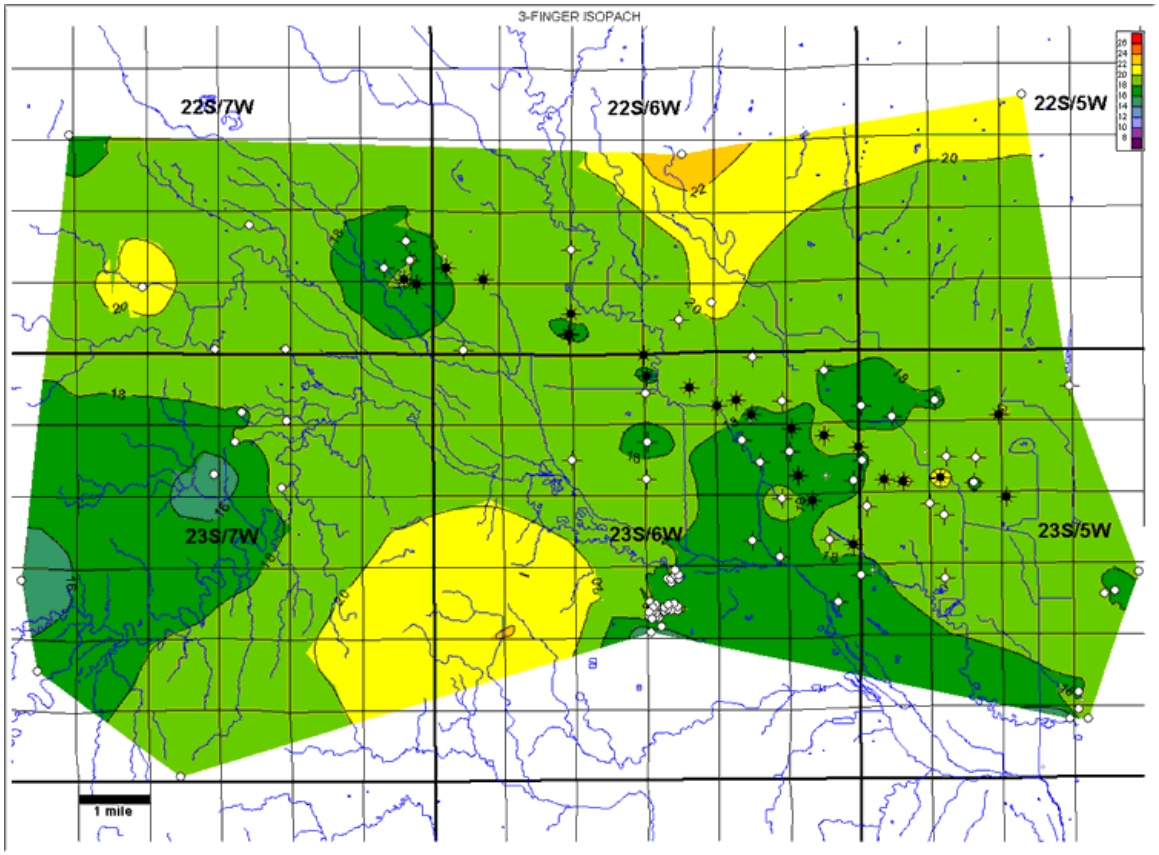

Figure 7A. Isopach map of the 3-finger dolomite interval. Contour interval = 2 ft. Wells within the study area not used in generating this map are displayed in gray at half size.

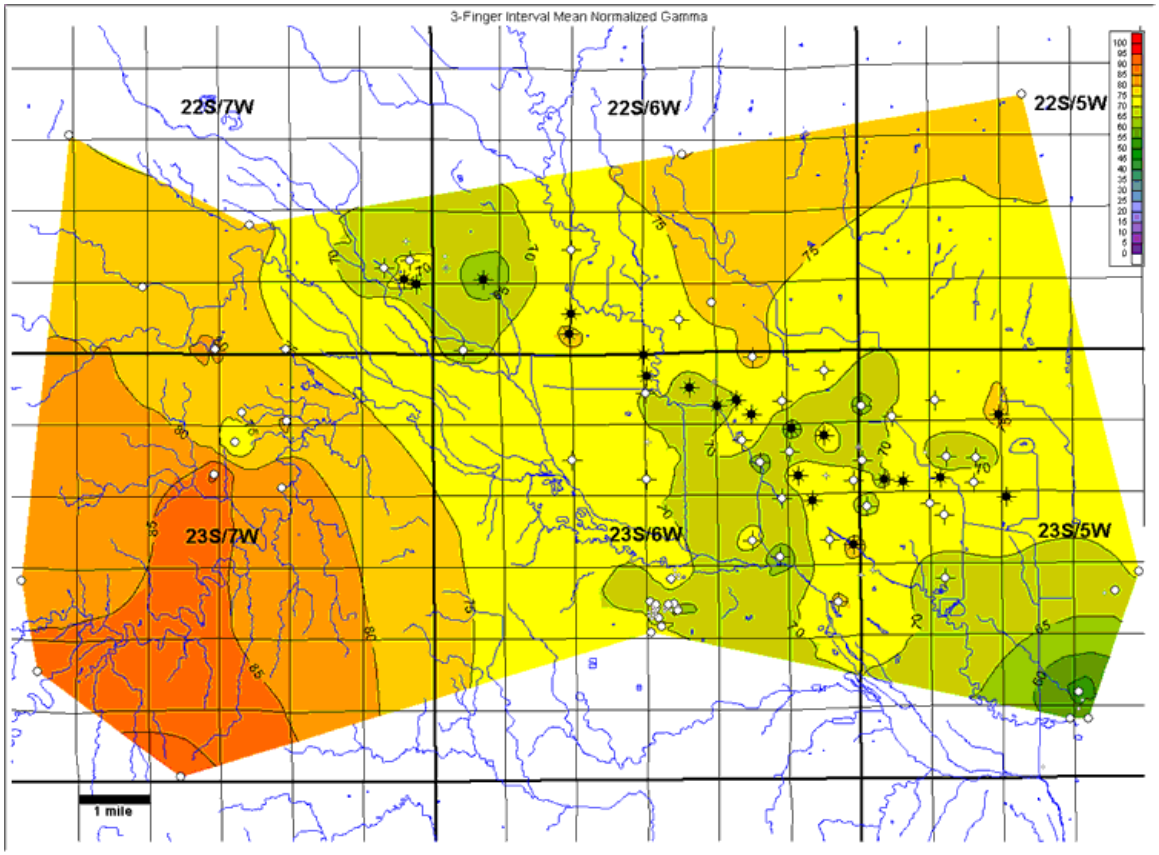

Figure 7B. Mean normalized natural-gamma ray for the 3-finger dolomite interval. Values are % shale. Contour interval = 5%. Wells within the study area not used in generating this map are displayed in gray at half size.

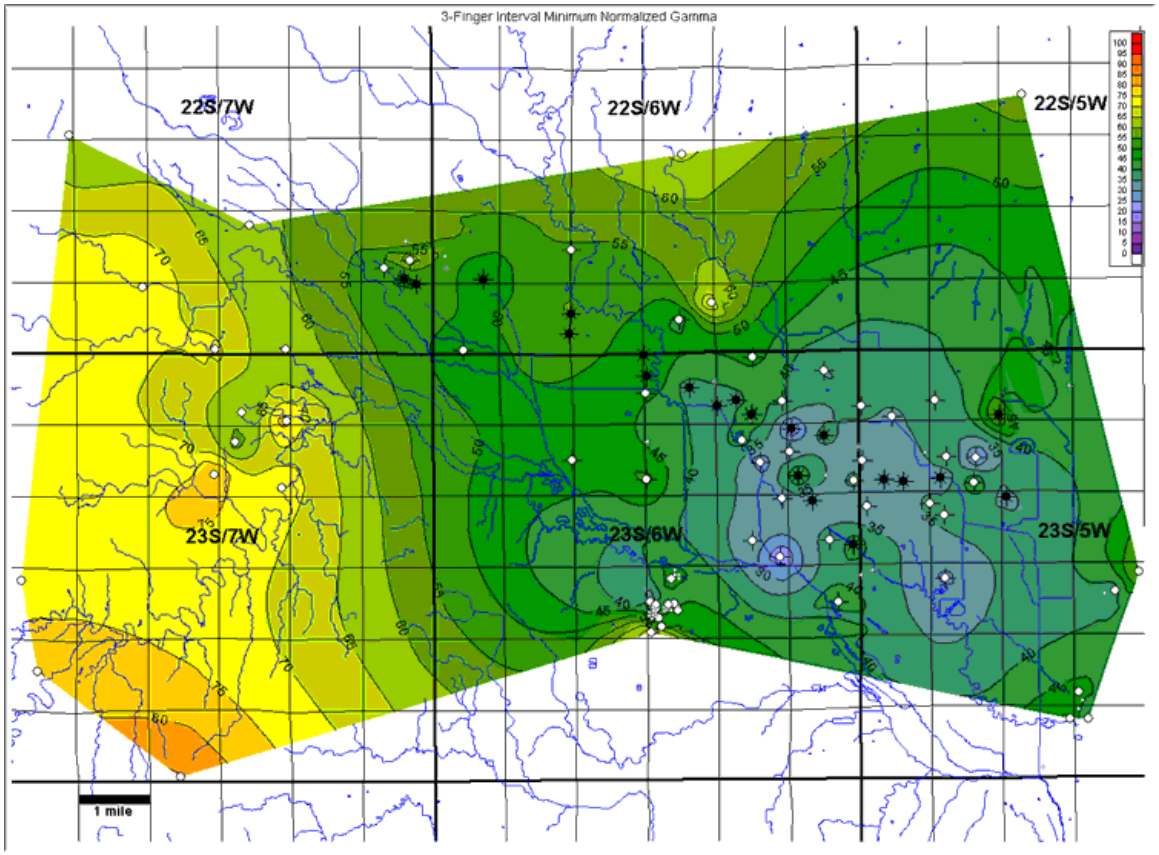

Figure 7C. Minimum normalized natural-gamma ray for the 3-finger dolomite interval. Values are % shale. Contour interval = 5%. Wells within the study area not used in generating this map are displayed in gray at half size.